Liquid Crystals
Publication details, including instructions for authors and subscription information:
http://www.informaworld.com/smpp/title~content=t713926090

A further experimental study of parallel surface-induced flexoelectric domains (PSIFED) (flexo-dielectric walls)

H. P. Hinov Corresponding author[a]; I. Bivas[a]; M. D. Mitov[a]; K. Shoumarov[a]; Y. Marinov[b]
[a] Laboratory of Liquid Crystals, Institute of Solid State Physics, Bulgarian Academy of Sciences, 1784 Sofia, Bulgaria [b] Laboratory of Biomolecular Layers, Institute of Solid State Physics, Bulgarian Academy of Sciences, 1784 Sofia, Bulgaria

Online publication date: 19 May 2010

To cite this Article Hinov Corresponding author, H. P. , Bivas, I. , Mitov, M. D. , Shoumarov, K. and Marinov, Y.(2003) 'A further experimental study of parallel surface-induced flexoelectric domains (PSIFED) (flexo-dielectric walls)', Liquid Crystals, 30: 11, 1293 — 1317
To link to this Article: DOI: 10.1080/02678290310001607198
URL: http://dx.doi.org/10.1080/02678290310001607198

LIQUID CRYSTALS, VOL. 30, NO. 11, NOVEMBER, 2003, 1293–1317

A further experimental study of parallel surface-induced flexoelectric domains (PSIFED) (flexo-dielectric walls)

H. P. HINOV*, I. BIVAS, M. D. MITOV, K. SHOUMAROV
Laboratory of Liquid Crystals, Institute of Solid State Physics, Bulgarian Academy of Sciences, 72 'Tzarigradsko Chaussee' blvd., 1784 Sofia, Bulgaria

and Y. MARINOV
Laboratory of Biomolecular Layers, Institute of Solid State Physics, Bulgarian Academy of Sciences, 72 'Tzarigradsko Chaussee' blvd., 1784 Sofia, Bulgaria

(*Received 7 January 2003; in final form 4 June 2003; accepted 21 June 2003*)

Parallel surface-induced flexoelectric domains (flexo-dielectric walls) have been further studied using new tools—a shadowgraph technique and computer processing of the most important images. It was unambiguously proved that the domains are a manifestation of the quadrupolar flexoelectric effect arising in a non-homogeneous electric field created by injection or by double electric layers. In the latter case they began to form at a d.c. voltage of 0.3–0.5 V. Furthermore, they arose near the injecting electrode and interfered with rubbing-induced domains at the junctions of every two adjacent domains. Flexo-dielectric walls have been obtained for the first time in the liquid crystal *p*-*n*-butyl-*p*-methoxyazoxybenzene and new experimental facts have been discovered. A new model for their creation is proposed.

1. Introduction

This paper describes the further study of parallel surface-induced flexoelectric domains (PSIFED) [1–6], also called flexo-dielectric walls, in MBBA nematic layers performed using new tools; namely the shadowgraph technique accompanied by computer processing of some of the observed images. We have obtained for the first time flexo-dielectric walls in the liquid crystal *p*-*n*-butyl-*p*-methoxyazoxybenzene (BMAOB), which is very similar to the liquid crystal Merck IV, and which displays strong flexoelectric properties. It is important to list the main non-flexoelectric instabilities and all the known types of flexoelectric domains in nematic liquid crystals having a small negative dielectric anisotropy, as well as to describe the known mechanisms leading to the creation of the instabilities. The main non-flexoelectric instabilities are:

(1) *Williams domains* [7, 8] (a first order θ-polar electro-convective instability). The polar θ-angle and the azimuthal ϕ-angle are shown schematically in figure 1 (for details see the text in § 4). The domains are perpendicular to the initial orientation of the liquid crystal.

(2) *Pikin domains* [9–12] (ϕ-azimuthal electro-convective instability arising in tilted nematic layers). The director can rotate around the axis OX (n_x = constant) or around the axis OZ (n_z = constant). The domains are along the initial orientation of the liquid crystal.

(3) *Injection-induced domains* (electro-hydrodynamic domains due to injected ions). The domains can be associated with a honeycomb or other, more complex form.

(4) *Relaxation hydrodynamic domains* discovered by Guyon *et al.* [13] and due to the Frederiks transition and the back flow effects. The domains are perpendicular to the initial orientation of the liquid crystal.

(5) *Static domains* due to the Fréedericksz transition [14]. The first discovered domains were parallel to the initial orientation of the liquid crystal. In general, they can be associated with various forms.

The flexoelectric instabilities are:

(1) *One-dimensional θ-polar flexoelectric domains* proposed by Meyer [15]. They should arise in a completely free flexoelectric nematic layer, and should be perpendicular to the initial

*Author for correspondence; e-mail: hinov@issp.bas.bg

Liquid Crystals ISSN 0267-8292 print/ISSN 1366-5855 online © 2003 Taylor & Francis Ltd
http://www.tandf.co.uk/journals
DOI: 10.1080/0267829031000160719 8

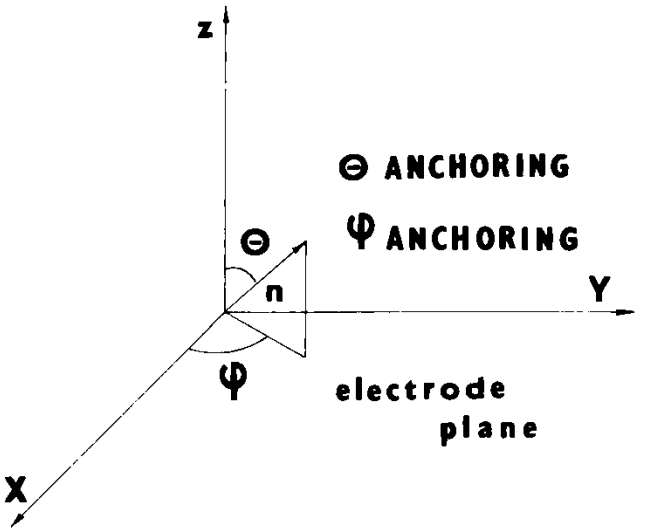

Figure 1. Schematic representation of the orientation of the director **n** at the surface, expressed by the θ-polar (zenithal) angle and ϕ-azimuthal angle. These angles determine the θ-anchoring and the ϕ-anchoring of the director **n**. The same representation of the director **n** can be used for every arbitrary point inside the liquid crystal layer.

orientation of the liquid crystal. These domains have been theoretically studied in a number of papers [16–18].

(2) *One-dimensional or two-dimensional θ-polar gradient flexoelectric deformations* discovered and studied by the Sofia Liquid Crystal Group in 1972–1974 [19, 20]. The gradient flexoelectric deformations have appeared in nematics with a small negative dielectric anisotropy (below 1) under the excitation of a gradient d.c. electric field. It was assumed that the inhomogeneity of the electric field is created by the bulk charges always present in the liquid crystal cells. Another very important requirement for the observation of such a flexoelectric effect was the existence of an initial tilt of the director, giving the mean orientation of the liquid crystal molecules along one preferable axis. The original differential equation given in [19] includes the gradient flexoelectric term and the dielectric term and has the form:

$$\Delta\theta - \left[\frac{(e_{1z}+e_{3x})}{K}\frac{\mathrm{d}E}{\mathrm{d}z} - \frac{\Delta\varepsilon}{4\pi K}E^2(z)\right]\sin\theta\cos\theta = 0 \quad (1)$$

where θ is the deformation angle, K is the mean elastic constant of the liquid crystal, $(e_{1z}+e_{3x})$ is the total flexoelectric coefficient, responsible for the bulk gradient flexoelectric torques and $\Delta\varepsilon$ is the dielectric anisotropy of the liquid crystal, which for the given case (MBBA) is negative. The validity of this equation was confirmed by the electro-optical measurements of nematic cells [19] On the basis of the gradient flexoelectric texturing of an MBBA nematic layer (compare figure 2a and figure 2b) Mitov [21] and Derzhanski and Mitov [22] have obtained experimentally for the first time the value of the total flexoelectric coefficient $(e_{1z}+e_{3x})$; see figures 2 (*a*) and 2 (*b*).

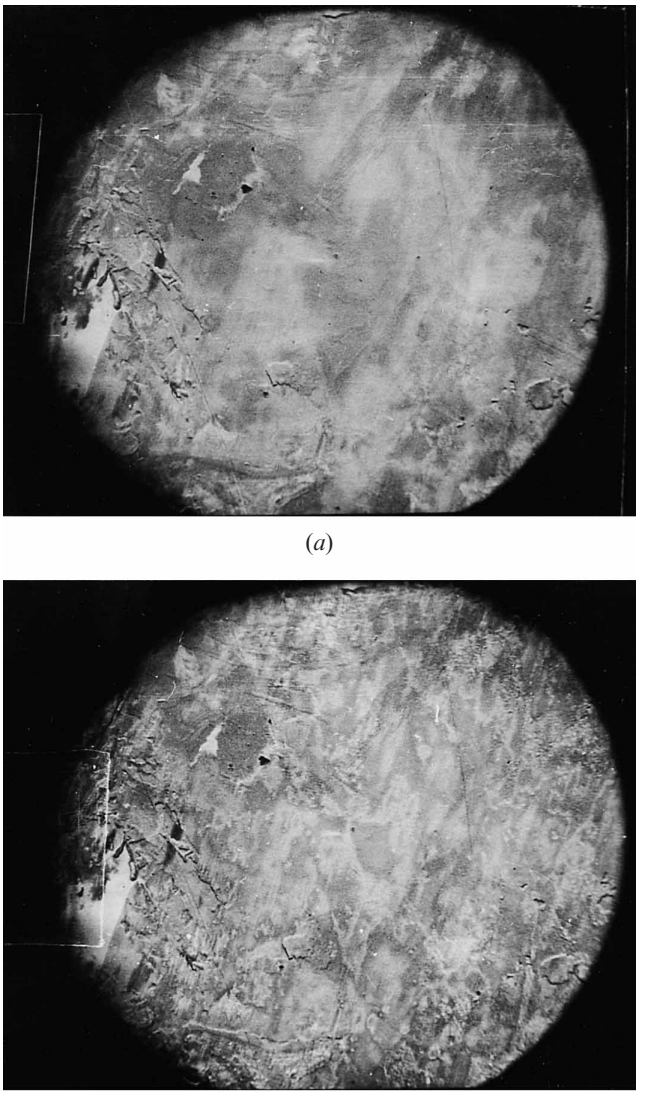

(*a*)

(*b*)

Figure 2. Interference-polarizing picture of a 30 μm thick planar MBBA nematic layer with weak anchoring (microscope MPI-5, differential regime, green light) [21]. (*a*) The type of initial deformations in the nematic layer when there is no applied d.c. voltage; (*b*) the type of gradient flexoelectric deformations, when a 4 V d.c. voltage is applied across the nematic layer.

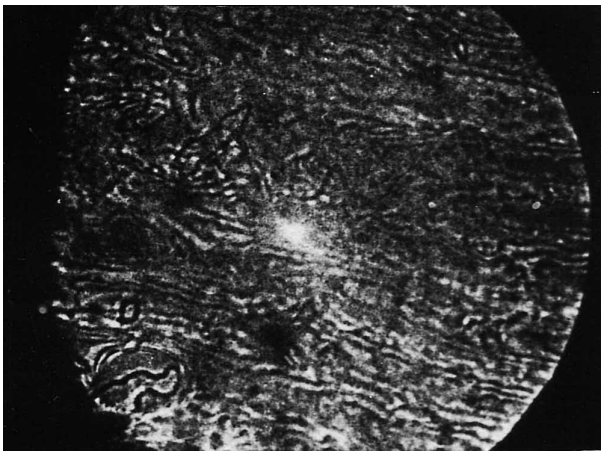

Figure 3. Periodic regime of the gradient flexoelectric effect in APAPA (anisylidene-*p*-aminophenyl acetate) with a thickness of 62 μm and applied 4 V d.c. voltage. The domain period is approximately 110 μm.

(3) *θ-Flexoelectric domains arising in a gradient electric field* [19, 20, 23, 24]. These are formed along the initial orientation of the nematic; see figure 3.

(4) *θ, φ-Volume flexoelectric domains* formed along the initial orientation of the nematic. They were observed by Vistin' in 1970 [25] and independently by Greubel and Wolff in 1971 [26]. Bobylev and Pikin [27, 28] have theoretically explained the flexoelectric nature of the domains discovered by Vistin' displaying both θ-poar and ϕ-azimuthal volume flexoelectric deformations. These authors have calculated the period of the domains and the threshold for their appearance, two important quantities which connect the material parameters of the liquid crystal with the value of the applied electric field. Many authors (see, for example [29–36]) have studied these domains.

(5) *Parallel surface-induced flexoelectric domains (PSIFEDs), or flexo-dielectric walls*, which are formed along the initial orientation of the nematic. The homogeneity of the electrode surfaces achieved, for example, by soap treatment (we have used a widely available commercial soap for washing) [1–5], or other surfactant [6] permits the creation of reproducible domains in nematics with a small (below 1) negative dielectric anisotropy and a weak polar-azimuthal anchoring of the liquid crystal (see figure 1). The domains usually appear near the cathode treated by soap or other surface-active substance. The PSIFEDs were experimentally studied either in symmetrical weak-anchored MBBA [1, 2, 5] or other nematic layers [5], or in asymmetrical strong–weak anchored MBBA layers [3, 4].

(6) *Rubbing-induced domains* transformed into *flexoelectric surface domains* on application of a d.c. voltage [37]. The rubbing-induced domains have been known for a long time. They are connected with the spatial treatment of the electrodes: rubbing followed by surfactant deposition. The combination of grooves and a surfactant usually leads to the observation of such domains. In our case they are connected with the spatial treatment of the electrodes: first rubbing with a diamond paste, then washing, rubbing with a soap and finally cleaning by rubbing with a cloth in the same direction [37]. They can be seen on some of the photomicrographs shown later.

It is very important to understand the mechanism generating the flexo-dielectric walls. The various instabilities are created by several mechanisms:

(1) The anisotropic Carr–Helfrich mechanism leading to the development of the well known electro-hydrodynamic domains of Williams [7, 8].

(2) The anisotropic Pikin's mechanism leading to the development of longitudinal electro-hydrodynamic domains [9–12] (we should point out that Pikin's mechanism is a modification of the Carr–Helfrich mechanism for tilted nematic layers and development of ϕ-azimuthal electro-hydrodynamic instability).

(3) The injection isotropic mechanism of Félici [38] leading to electro-hydrodynamic domains in the nematic and isotropic phases of the liquid crystals (see, for example, [39–48]). It is well known that the injection exists at a d.c. voltage or at a very low frequency voltage [45] (see also [49], figure 7).

(4) The electrolytic isotropic mechanism leading to electro-hydrodynamic domains in the nematic and isotropic phases of the liquid crystal. This mode exists at a low frequency range (see [49], figure 7).

All the instabilities listed are hydrodynamic. It is important to mention, however, that around the threshold the velocity of the fluid is usually very small and one can erroneously conclude that these are static instabilities [48, 50, 51]. From the mechanisms listed one should exclude the electrolyte mechanism (the flexo-dielectric walls cannot be formed at a frequency above 1 Hz). As far as the injection mechanism is concerned, it will be considered later in a separate paragraph describing the similarities and differences between the flexo-dielectric walls and the

injection-induced domains. The Carr–Helfrich mechanism and Pikin's mechanism will be taken into account in developing a model, explaining qualitatively the appearance of the flexo-dielectric walls.

The new tools used here to study flexo-dielectric walls, namely, the shadowgraph technique and the computer processing of some of the observed images (see later), provide very important information about the region of development of the flexo-dielectric walls. Our experimental results have unambiguously shown for the first time that the flexo-dielectric walls in MBBA nematic layers arise near the cathode and that they penetrate to the electrode only at the junctions of the walls. This very important experimental fact was evidenced by the clear separation of the rubbing-induced domains [37] situated on the electrode, and the flexo-dielectric walls arising above them in the cathode region. One can also see the penetration of the inverse walls [52] terminating on the glass plate with inverse surface lines [52, 53]. The shadowgraph technique provided, on the other hand, experimentaly proof that the flexo-dielectric walls can appear even at 0.5 V, a fact which has not before been published, and that the electrochemical behaviour of the nematic MBBA can enhance these domains [54–59].

This paper is organized as follows: in § 2 the requirements for the observation of flexo-dielectric walls and their typical properties are given. In § 3 part, the similarities and differences between flexo-dielectric walls and injection-induced domains are also given. In § 4 we clarify some details concerning the preparation of the experiment; in § 5 and § 6 we describe experimental results obtained using the shadowgraph technique and the computer processing of some of the obtained images. In this section new facts are mentioned concerning the electro-optical behaviour of the liquid crystal BMAOB, including the separate observation of the flexo-dielectric walls and the flexo-electric domains of Vistin' *et al*. The paper finishes with a discussion of the experimental results obtained and the proposal of a new model that qualitatively explains the appearance and development of the domains. This model is based on experimental observation of the flexo-dielectric walls and on the experimental results, ideas and models proposed by other authors.

2. On the requirements for the observation of flexo-dielectric walls, the main properties and their absence

The requirements for the observation of the flexo-dielectric walls under a d.c. voltage excitation are [60]: (a) the existence of non-vanishing flexoelectric coefficients; (b) a small negative dielectric anisotropy below 1 (this is only a suggestion, these domains should be obtained also in nematics with a large dielectric anisotropy); (c) A relatively large conductivity of the liquid crystal: $\sigma \sim (10^{-8}\text{–}10^{-9})\,\Omega^{-1}\,\mathrm{cm}^{-1}$ (experimental results with the liquid crystal BMAOB show that these domains can arise also in less conductive nematics); (d) a weak polar-azimuthal anchoring of the liquid crystal at least at one of the boundaries (for example, the glass plate), see figure 1, for details see § 4; (e) a relatively good initial orientation of the liquid crystal with low, middle, or high tilt (there are no experiments with a stabilizing magnetic field and it is not known whether these domains would arise in a perfectly planar nematic layer); (f) absence of other types of domains in the region of the liquid crystal where the flexo-dielectric walls have been formed; (g) application of a d.c. or very low frequency voltage (theoretically below 2 Hz, experimentally below 0.2 Hz, depending on the value of the voltage and the thickness of the liquid crystal layer); (h) a current flowing through the cell.

The typical properties of flexo-dielectric walls are (most of these properties have been obtained in other papers [1–6], some in this paper):

(1) They arise at a threshold voltage (more correctly at an optical threshold voltage) of 2–3 V coinciding with the voltage of the chemical degradation of the liquid crystal, for example MBBA [55, 57]. In some cases, however (see the experimental results later), the domains appear at a voltage of 0.3–0.5 V, which coincides with the formation of electrical double layers.

(2) A decrease of the threshold voltage from 6 V ($d = 5\,\mu\mathrm{m}$) to 3 V ($d = 90\,\mu\mathrm{m}$) for the case of symmetric weak anchoring [2], where d is the thickness of the liquid crystal cell; or from 10 V ($d = 9\,\mu\mathrm{m}$) to 1.5 V ($d = 150\,\mu\mathrm{m}$) for the case of strong–weak anchoring [4]. (The decrease of the thickness of the cells naturally leads to an increase in the threshold voltage due to mutual interactions between pairs of adjacent domains, representing flexo-dielectric walls. On the other hand, the injected ions must be replaced by ionic impuritie on increasing the thickness of the nematic cells under study, i.e. the ionic conductance should be changed to an ohmic one. These causes evidently lead to a decrease in the threshold voltage for the thicker cells.) Here we must mention that there is a cut-off thickness above which the domains disappear (for instance 90 μm [2] for symmetrical weakly anchored MBBA nematic layers). For the case of asymmetrically strong–weak anchored nematic MBBA layers this thickness is greater than 200 μm [4] (the exact value is not known). There is also a minimum thickness which was observed only for

the case of the liquid crystal BMAOB and was measured to be in the range 6–7 μm.

(3) A decrease of the ratio p/d, where p is the period of the domains, from 3 (thin cells) to 1.5 (thick cells) [2, 4].

(4) The domains arise in the form of walls around the threshold.

(5) Above the threshold (typically around 4 V, a voltage probably coinciding with that for the injection domain [39–41], the domains are transformed into electro-hydrodynamic domains.

(6) The form of the domains drastically changes with the value of the initial tilt of the liquid crystal layer, the thickness of the liquid crystal cell, the anchoring of the liquid crystal and the thickness of the soap layer ensuring the weak anchoring. Up to now one distinguishes the following kinds: (a) cross-like domains which arise in homeotropic layers and relatively thick soap layers [2]; (b) cross-like domains and π-walls usually terminating with two point disclinations [53] in high-tilted nematic layers (see figure 4, H.P.Hinov, unpublished results), it is curious that the π-walls did not change their type under crossed polarizers at their random orientation in the XY plane; (c) flexoelectric, predominantly θ-walls, arising at a relatively high tilt of the liquid crystal (see figure 5), for details see the experimental results described in [2]); (d) flexoelectric θ,ϕ-walls arising at a moderate tilt of the liquid crystal layer (see figure 6), for details see the experimental results described in [1–5]).

(7) When the thickness of the soap layer is of the order of one to several soap molecules one observes domains, very similar to the flexo-dielectric walls (with a small azimuthal ϕ-deformation). The only difference is that in the region of the wall junctions there is a hydrodynamic movement of the fluid (see figure 4 in [4]) while the threshold and the period of the domains have not changed. Furthermore, these domains can be easily removed with an additionally applied a.c. voltage with a frequency above the cut-off value, for example 10 V, 20 kHz when $U_{DC} = 3.5$ V.

(8) The simultaneous application of a d.c. voltage and a high frequency voltage with a frequency above the cut-off leads to the disappearance of the flexoelectric deformations. First the polar

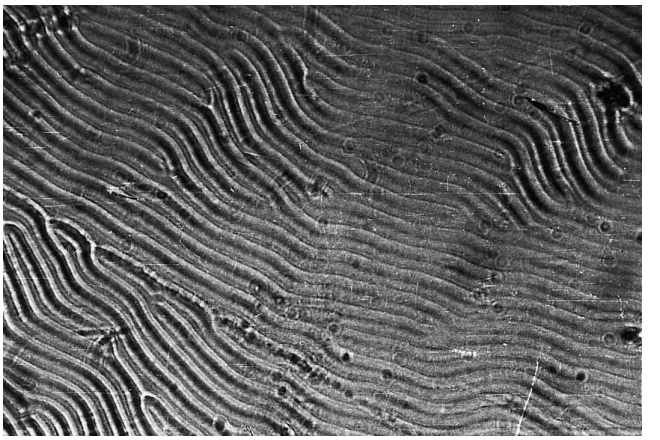

Figure 5. Longitudinal domains (flexo-dielectric walls) in a MBBA nematic layer with a thickness of 15 μm and symmetric weak anchoring, an applied d.c. voltage of 7 V, magnification 12.5 × 12.5, the period of the domains is 27 μm.

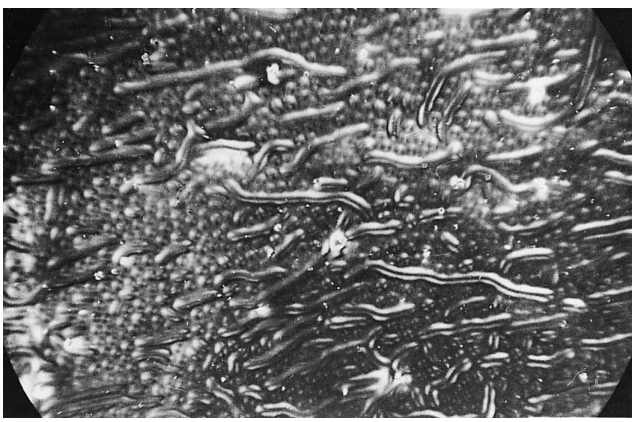

Figure 4. Cross-like domains and π-walls in MBBA nematic layer with a thickness of 42 μm, crossed polarizers, an applied d.c. voltage of 4 V, magnification 6 × 10, the long side of the photo corresponds to 1350 μm.

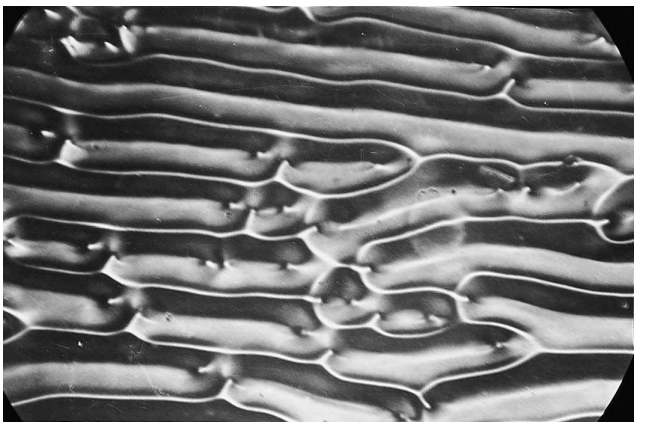

Figure 6. Longitudinal domains (flexo-dielectric walls) in a MBBA nematic layer with a thickness of 30 μm and asymmetrical strong–weak anchoring, an applied d.c. voltage of 6 V, A 30° $\mathbf{n}_0$ 0° P, magnification 6 × 10, the long side of the photo corresponds to 1350 μm.

θ-deformations disappear; these are usually concentrated in the regions of the wall junctions terminating with surface disclinations, for example 4–20 V, 10 kHz, when $U_{DC} = 3$–8 V. The azimuthal ϕ-deformations which are in the rest of the cell disappear at higher voltage, for example $U_{AC} = 100$–170 V. The domains can be removed with a small a.c. voltage, in the range 6–12 V, when they are in the form of θ-walls.

(9) The flexo-dielectric walls disappear at the spacers or around bubbles [5]; it is not clear, however, whether the lateral boundary conditions or the lack of ions in these regions are responsible for this disappearance.

(10) A strong non-homogeneous electric field in the whole liquid crystal layer removes the flexo-dielectric walls [5].

(11) In the case of the liquid crystal MBBA, flexo-dielectric walls are always formed near the cathode (this fact can be proved by changing the focusing). Our new experimental results obtained with the liquid crystal BMAOB clearly show that the flexo-dielectric walls can also be obtained at the anode.

(12) A change of polarity of the applied d.c. voltage initially enhances the flexo-dielectric walls, followed by the gradual disappearance of the walls in the presence of strong–weak anchoring. In the case of symmetric weak–weak anchoring the flexo-dielectric walls reappear at the other soap-treated electrode. The duration of this dynamical behaviour crucially depends on the thickness of the liquid crystal layer and the strength of the electric field (for details see the results given in [2]).

(13) Flexo-dielectric walls can easily be obtained after switching the liquid crystal from dynamic scattering to the domain mode, which evidently leads to the presence of more ions and therefore to a stronger electric field gradient near the electrodes. The presence of ions in the liquid crystal cells is so important that the application of an a.c. electric field with a large amplitude, an appropriate frequency and a short duration can transform the Williams domains into longitudinal domains [61] of the Pikin type [9–12] (according to the authors of this paper). In our opinion, the gradient flexoelectric effect leads to the tilt of the nematic and to the development of the Pikin domains.

(14) In the case of pure nematic MBBA layers with a cut-off frequency 50–60 Hz (conductivity around $10^{-11}\,\Omega^{-1}\,cm^{-1}$), the domains appear only close to the nematic–isotropic phase transition, i.e. in a temperature interval of several °C below the clearing point (H.P.Hinov, unpublished results).

(15) The domains are hardly recognizable under application of rectangular voltage pulses (H.P.Hinov, unpublished results).

(16) Close to the threshold and slightly above it the flexo-dielectric walls are static (this can be shown by immersion of fine particles in the fluid or by the behaviour of small nematic droplets embedded in the isotropic phase of the liquid crystal (for details see the comments in [41]).

(17) The optical form of the domains is very peculiar (see § 6, § 7 and text later).

Flexo-dielectric walls cannot exist when: (a) the anchoring of the liquid crystal at both glass plates, for a liquid crystal cell of a sandwich type, is strong; (b) the anchoring of the liquid crystal is vanishingly small; this experimental situation can be achieved when the two glass plates are treated by a thick and rubbed soap layer; (c) the liquid crystal is very pure (this depends on the value of the conductivity).

3. A comparison of injection-induced domains and flexo-dielectric walls: similarities and differences

The electro-optic behaviour of nematic liquid crystal layers exposed to a d.c. voltage excitation is of great importance for their application in practice. This behaviour, however, can be significantly complicated by the formation of double electric layers, followed by injection of ions from one or both electrodes. This injection leads in many cases to the appearance of various kinds of domains at a relatively small value of the d.c. voltage applied across such cells. For example, Koelmans and van Boxtel [39, 41] and the Orsay Liquid Crystal Group [40] have observed injection-induced domains in the liquid crystal MBBA. The threshold voltage showing the appearance of these domains was around 5 V, while the time of response was in the range of hundreds of milliseconds [39, 41]. Injection-induced domains are now well known [7, 42] and have been explained theoretically by Felici [38]. It should be noted, however, that the mechanism of the creation of these domains is isotropic and the hydrodynamic movement of small particles dispersed in the fluid can be observed not only in the nematic phase but also in the isotropic phase [7, 38–47].

In comparison with the well known Williams domains, governed by the anisotropic Carr–Helfrich mechanism [7], injection domains are very complex. Their type depends critically on the electrode surface and can be hexagonal, linear or intermediate [40]. Such domains have usually been obtained and studied when

the anchoring of the liquid crystal at the limiting boundaries is strong. It has been pointed out in the literature that the anisotropic Carr–Helfrich mechanism cannot be applied in this particular case [39–41, 62]. On the other hand, a rise in the value of the applied d.c. voltage can considerably enhance the value of the electric field in the double electric layers at the electrodes [63–65], which in its turn enhances the injection. Injection domains are also important in relation to electrochemiluminescence in electrolyte-containing or electrolyte-free solutions [66]. Injection in such cells is connected with the electrochemical behaviour of the fluid and can lead to the appearance of domains even at a d.c. voltage of 3 V [66].

Felici proposed a mechanism for the creation of injection-induced domains [38]. The experimental data, however, are quite contradictory and confusing. For example, leading authors in this area [40, 44–46, 58] (see also the cited papers in [2]) claim that injection from the electrodes is impossible in highly conductive nematic or isotropic liquids, whereas flexo-dielectric walls have usually been observed in such fluids. According to these authors, in highly conductive liquids with conductivity in the range 10^{-7}–$10^{-8}\,\Omega^{-1}\,cm^{-1}$, the contribution of injection to the total current is very small compared with the ohmic contribution. According to other authors however [45, 58], the increase of the conductivity (e.g. by doping the nematic with ionic substances) enhances the value of the electric field at the electrodes due to electrical double layers, and greatly facilitates the injection [39, 58, 66]. Furthermore, there are examples of contradictory results between theory and experiment about the place of appearance of the injection domains. It is also unclear which type of the injection, unipolar [42] or bipolar [44], favours the appearance of injection domains, for example, in a conventional MBBA cell [39–41]. The experimental observations described in [1–5] and the experimental study in this paper clearly show that for the particular case of nematic MBBA, soap treatment of the electrode favours injection from the cathode only. Later we shall show that in the case of the liquid crystal BMAOB, soap treatment of the electrodes does not affect injection from either electrode.

There are similarities and differences between flexo-dielectric walls and injection-induced domains. The form of both types of domain depends critically on the surface of the electrodes. They can be linear, intermediate or hexagonal [1–5, 40], and were all observed during our experimental study. One must stress, however, that flexo-dielectric walls show these forms through the orientation of the director itself, whereas the patterns connected with injection-induced domains are simply focal lines visualized by the flow birefringence [40]. Certainly one can find examples where only injection domains exist, or when the forms of the flexo-dielectric walls and the injection domains are the same. For example, we have observed only injection domains, very similar to those already observed by the Orsay Liquid Crystal Group [40] and by Durand *et al.* [48] (the so-called twin-domains with twin-rotator flows). They were obtained in nematic MBBA layers when one of the glass plates was treated with soap and the other had been coated using vacuum SiO evaporated ensuring a highly tilted orientation followed by lecithin deposition (we do not show these results in this paper).

The homeotropic alignment of the director at this boundary does not permit the formation of flexo-dielectric walls. On the other hand, it is well known that injection domains are very often hexagonal or honeycomb. In experiment we have observed the formation of similar static flexo-dielectric walls when the director is highly tilted at the boundaries. The increase of the d.c. voltage to 4–5 V led to the appearance of hydrodynamics within the hexagons or the honeycombs, especially in regions where the ions are concentrated, namely the adjacent sides of the domains, while the form of the domains did not change (we do not describe these results in this paper). The flexo-dielectric walls, however, are usually longitudinal and static around and slightly above the threshold. One can usually transform the longitudinal domains into hexagonal or honeycomb domains on increasing the voltage. It is evident that the appearance of the domains is very complex and depends critically on the treatment of the electrodes, the distribution of the ions inside the liquid crystal layers, the value and the frequency of the applied voltage and, finally, the existence of other static or hydrodynamic instabilities. Another very important similarity between flexo-dielectric walls and injection domains is that both arise at unipolar or bipolar injection. There is, however, one exception: flexo-dielectric walls can also arise at the formation of electrical double layers with the participation of impurity or other ions in the bulk of the liquid crystal. The appearance of flexo-dielectric walls at a voltage of 0.5 V (see the experimental results later) supports this view.

There are several important differences between flexo-dielectric walls and injection-induced domains. The first, and perhaps the most important difference, is that the appearance of injection domains is accompanied by a considerable rise in current flowing through the studied cells [43]. Inversely, the current does not change at the appearance of flexo-dielectric walls. Further, injection domains can be easily removed by an additionally applied a.c. voltage with a frequency

above the cut-off for the dielectric relaxation of the ions. For example, injection-induced domains, developed well above the threshold, can be removed with an a.c. voltage of 6–8 V. In contrarst, flexo-dielectric walls even slightly above the threshold, say 3.5 V, can be removed by a voltage in the range 50–170 V depending on the form of the deformations. In rare cases this voltage decreases to 8–12 V when θ-polar deformations in the flexo-dielectric walls prevail. Another important difference is that injection domains usually appear at the collector when the applied voltage is d.c. [43]. Inversely, flexo-dielectric walls usually appear at the injecting electrode. We should point out, however, that flexo-dielectric walls can be formed also at the collector. This is due to the large difference between the true, electrochemical velocity of the ions and their hydrodynamic velocity, which is several orders of magnitude higher. Finally, injection domains and flexo-dielectric walls behave differently under the application of a magnetic field oriented parallel to the initially applied electric field [1, 40]; for further information see [2].

Although flexo-dielectric walls were discovered in 1978, a number of questions regarding their nature still need to be clarified. Specifically, the experimental data are insufficient to prove unambiguously their flexoelectric character and also, a clear model is lacking which can explain the role of flexoelectricity in their appearance. In order to obtain new experimental data, we decided to use new tools for their study and new materials displaying strong flexoelectric properties. The important new experimental results obtained and discussed in this paper, together with experimental results obtained by other authors [33, 34] allowed us to reconsider some theoretical ideas and results [3, 4] based on the theoretical explanation of Vistin' *et al*. [25, 26] elaborated by Bobylev and Pikin [27, 28]. New ideas for the development of these domains, based on the recent new experimental observations are given at the end of this paper.

4. The preparation of the experiment

4.1. *Preparation of the liquid crystal cells*

The electro-optic properties of liquid crystals, and particularly of nematic liquid crystals, are usually studied with cells or samples consisting of two flat glass plates covered with semitransparent conductive layers separated by two isolation sheets of Teflon or some other polymer. These sheets determine the thickness of the liquid crystal cells; wedge-like cells have been also used. Cells prepared in this manner permit the study of the properties and electro-optical effects in nematics of variable thickness. The liquid crystal cells are usually sealed with a material inert to the liquid crystal substance in order to avoid contamination of the liquid crystal.

4.2. *Methods of study and experimental set-up*

Sandwich liquid crystal cells are usually studied under a polarizing microscope which can work in two regimes: a *birefringent regime* when two nicols (polarizer and analyser) are used or a *shadowgraph regime* when only a polarizer is used. The latter regime is sometimes called a *regime of contrasts*. The shadowgraph technique is widely used for the study of electro- and thermo-dynamic instabilities in various fluids, including liquid crystals [67–70]. A standard shadowgraph set-up is usually used for the study of electroconvection. Light is focused by the director variation either in the XZ plane (polarization of the light along the OX axis) or in the YZ plane (polarization of the light along the OY axis). It is clear that the shadowgraph regime does not permit visualization of the ϕ-deformation; in the birefringent regime, however, one can observe bulk θ,ϕ-deformations [70, 71]. Additionally one can use a $\lambda/4$ plate which permits identification of $+\phi$- and $-\phi$-deformations [71].

During optical observations, a collimated beam of light, polarized usually perpendicular to the initial orientation of the liquid crystal, traverses the cell along the direction of the electric field. The resulting image is acquired with a charge-coupled device (CCD) camera attached to a microscope and digitized by a frame grabber with a spatial resolution of 512×512 pixels, 256 grey levels, which corresponds to 8 bits. The digitized images are stored and processed on the computer 'Pentium' 133 MHz (32 micro B RAM) by one-dimensional Fourier optical analysis. The area of each pixel depends on the magnification of the polarizing microscope and the attached additional optical technique. For example, the dimensions of the pixel varied between $1 \times 1\,\mu m^2$ and $0.5 \times 0.5\,\mu m^2$. This accuracy was relatively good since it corresponds to the optical resolution of the polarizing microscopes used in our experiment. All the Fourier analysis (FA) curves shown later are spectral densities (arbitrary scale) plotted against the reciprocal wavelength (cm^{-1}).

4.3. *θ, ϕ-Angles and θ, ϕ-anchoring of the director (see figure 1)*

In general, the position of the director (the mean orientation of the liquid crystal molecules along one preferred direction) can be represented by two angles: the polar (or zenithal) angle θ and the azimuthal angle ϕ (see figure 1). The θ-deformations in one nematic layer, on the stage of a polarizing microscope, can be easily observed when the initial axis of alignment of the

liquid crystal is along the bisectrix of the crossed polarizer and analyser. Conversely, ϕ-deformations can be easily observed when the axis of the initial alignment of the liquid crystal is oriented either along the analyser or along the polarizer when they are crossed, and the sample is rotated to $+\phi$ or to $-\phi$. In the shadowgraph regime, one cannot see the azimuthal ϕ-deformations. Additionally, one can define separately the θ-polar and the ϕ-azimuthal surface energies. For the case of tilted nematic layers, however, the situation is more complex since in this case these two variables are coupled. This case was first considered by Jérôme [72] when the two strength constants W_θ and W_ϕ are equal:

$$W_s = -\frac{1}{2} W_s (\mathbf{n}.\mathbf{n}_0)^2 \quad (2)$$

where $\mathbf{n}_0$ is along the initial orientation of the liquid crystal. This surface energy is a nonlinear combination of the azimuthal and polar angles [73]. The most general form of the surface energy, when the θ- and ϕ-strength constants are unequal, has been obtained by Beica *et al.* [74]:

$$W_s = \frac{1}{2} W_\theta \{[\mathbf{n}_0 \times (v \times \mathbf{n}_0)].\mathbf{n}\}^2 + \frac{1}{2} W_\phi [(v \times \mathbf{n}_0).\mathbf{n}]^2 \quad (3)$$

The orientation of the two polarizers with respect to the flexo-dielectric walls is of great importance for understanding the orientation of the nematic director itself. For example, the Williams domains are usually investigated with a polarizer oriented along the initial alignment of the liquid crystal (usually coinciding with the OX axis) while longitudinal domains such as the observed flexo-dielectric walls should be studied with a polarizer oriented in the perpendicular direction, i.e. in direction of the OY axis. In some cases, however, the liquid crystal deformations are more complex and one should use some other orientations of the two polarizers. The bulk θ, ϕ-deformation of the liquid crystal can be clarified by the mutual orientation of the domains and the polarizer in the shadowgraph regime, and the mutual orientation of the domains and the two polarizers in the birefringent regime.

4.4. *Liquid crystals, preparation of the electrodes and a voltage source*

The electro-optical effects in liquid crystals are usually studied after the application of a d.c. or a.c. voltage, or in some cases after the application of both. The electro-optical response of the liquid crystal cells depends on the elastic, dielectric, flexoelectric and optical properties of the liquid crystal. The electro-optical response also depends on the forces of interaction between the liquid crystal and the confining walls. The strength of the surface torques depends critically on the surface energy of interaction between the liquid crystal and the substrates. In our experiment we used the well known and widely studied liquid crystal MBBA (*p*-methoxybenzylidene-*p*-*n*-butylaniline) [8]. In order to check the appearance of flexo-dielectric walls in one typical flexoelectric substance we chose the liquid crystal BMAOB (*p*-butyl-*p*-methoxyazoxybenzene) with a nematic phase in the range 21–73°C and a small negative dielectric anisotropy measured at between -0.2 and -0.25 [29, 36]. The elastic constants of this liquid crystal have also been measured [75, 76]. This liquid crystal is a mixture of two isomers [36] and is very similar to the liquid crystal produced by Merck known under the name Merck IV or N4 [26, 30]. The only difference is in the ratio of the two isomers: 60 versus 40 wt %, and the reverse.

Flexo-dielectric walls, as noted, appear when there is weak anchoring of the liquid crystal at least at one of the two electrodes. It is well known that weak anchoring of the liquid crystal can be easily achieved when the electrodes are treated by a surface-active substance, e.g. by soap [1–5]. The thickness of the soap layer should be below 0.1 μm [37]. Fortunately, the liquid crystal BMAOB can also be influenced by soap treatment of the electrodes and the anchoring, as in the case of MBBA, is also weak. This is not surprising since part of the BMAOB molecule is very similar to that of MBBA (strongly polar liquid crystals, such as biphenyls however, are only weakly influenced by soap treatment of the electrodes). Current and previous investigations of the soap layers, give no answer as to the causes for the achievement of this weak interaction between the liquid crystal and the soap-treated wall [77–79]. We shall try to explain this behaviour only qualitatively.

First, the mechanical treatment of the soap evidently leads to good homogeneity of the soap layer in the treated regions (compare with the AFM pictures presented in figure 1 of the [79] for the case of one non-treated soap layer). Second, the first monomolecular layer of the soap is strongly attached to the metal or to the semiconductor, ensured by chemical bonds between the polar groups giving the stability of the soap layer, whereas weak anchoring is ensured by long range van der Waals interactions between hydrocarbon chains and liquid crystal molecules [78]. It should be pointed out that multilayers of polar compounds several hundred nanometers in thickness have been observed between metal surfaces under certain circumstances [80]. Furthermore, it had been reported that these films posses liquid properties with long range ordered structures (now it is well known that such multilayers of soap molecules can form smectic liquid crystalline phases). Such films are resistant to normal pressure up to 400 kPa. Once sheared however, they

readily lose thickness, thereby minimizing their effectiveness as multilayer films [78, 80]. This, however, is not valid for our case since the soap layer is initially very thick, probably hundreds of microns, and after the rubbing the thickness drastically reduces below 0.1 μm (in some cases below 0.01 μm), the range of the depth of mechanical scratching of the glass plates [37].

The strength of liquid crystal–soap interactions are dictated, by the density of the soap molecules [77] and by the existence of holes in the soap layer [81]. It is evident also that a thick soap layer screens the molecular short range forces acting on the first soap molecular layer on the glass plate, and only long range dispersive molecular forces are responsible, as noted above, for the weak interaction of the liquid crystal with the rest of the soap layer [82]. The lack of various elastic walls arising at very weak surface anchoring [82, 83], and the strong thermal fluctuations of the director [84] (all our experiments are performed at room temperature) clearly show that the surface anchoring of the liquid crystal is in the range of $10^{-3}\,\mathrm{erg\,cm^{-2}}$ (see also the discussion in [37]).

Soap deposition is achieved by special treatment of the electrodes which are initially rubbed with a diamond paste applied on a cloth, cleaned with acetone or other organic liquid, dried, rubbed with dry soap in the same direction and then rubbed again with a clean cloth in the same direction. From the experimental results we know only that the rubbing itself determines (a), a small tilt (relative to the unit normal vector) of the director, presumably in the direction of rubbing (figure 7), and (b), that the rubbed soap layer determines very weak θ, ϕ-anchoring of the liquid crystal (figure 1, see § 4.3).

The θ-polar (or zenithal) surface energy can be estimated from the thickness of the θ-surface disclinations [85–87]. Such disclinations can be easily observed in semi-free nematic layers spread on a glass plate treated by a thick soap layer [37]. This surface energy can be additionally estimated from the Fréedericksz threshold. The azimuthally ϕ-surface energy can also be estimated from the thickness of the ϕ-surface disclinations [85–87] or by the electro-optical behaviour of a twisted layer when one or both glass plates are treated with soap. We have estimated in [37] that the surface energy is in the range of $2\times10^{-3}\,\mathrm{erg\,cm^{-2}}$. The initial tilt of the director is due to the inhomogeneity along the rubbing direction (see figure 7) [37]. The structure of the soap layer, at the present stage of the experimental study, is unclear; although X-ray scattering from thin multilayer films of soap did shed some light on the soap organization in such layers [79]. The rubbing of the soap can drastically change this organization and eventually the alignment of the soap molecules; further study in this direction is needed.

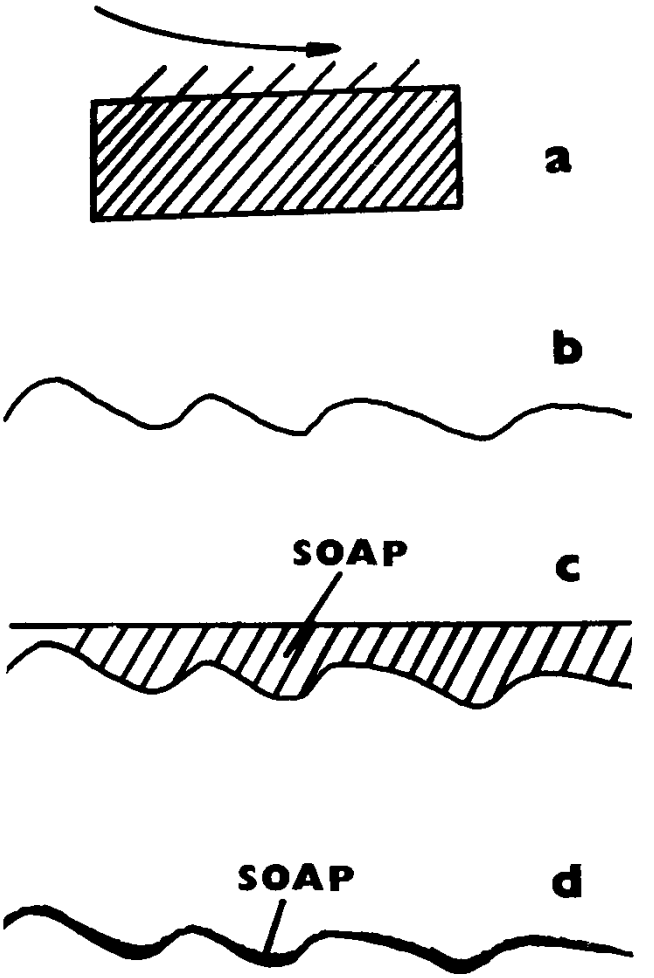

Figure 7. A schematic representation of the process of soap deposition and the sign of the initial tilt connected with small period undulations of the surface along the rubbing direction.

The application of the d.c. voltage was in steps of amplitude 0.14 V and duration 30 s. In some cases, the voltage was increased by several steps; it could reach 7 V in 50 steps. The liquid crystal BMAOB was studied under a polarizing microscope in the usual birefringent regime and with the application of d.c. or d.c. and a.c. voltages. Two kinds of liquid crystal cell were prepared. The first was with asymmetrical strong–weak anchoring. The strong anchoring was achieved by rubbing on a thick polyvinyl alcohol layer with a thickness of hundreds of microns, serving as an orienting layer [88]; according to some authors [89] such a polyvinyl alcohol layer can electrically block the electrodes. The weak anchoring was obtained by soap treatment of the second electrode. The second kind of cell, studied only

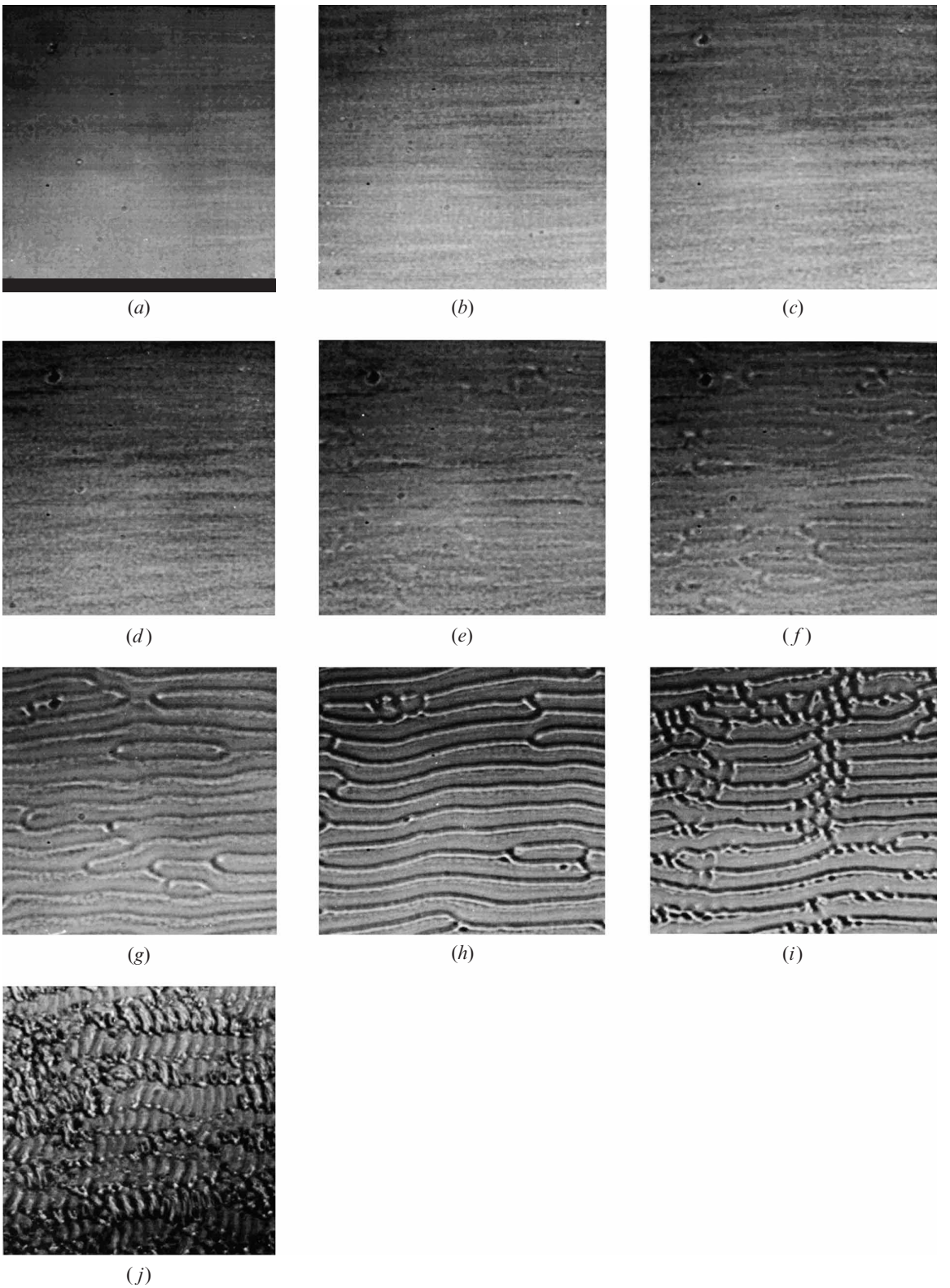

Figure 8. A number of photogrophs taken from laser-printed images showing the appearance and development of longitudinal domains (flexo-dielectric walls) in a 12 μm thick nematic MBBA layer with weak anchoring at both electrodes achieved by soap deposition. The polarizer is oriented perpendicular to the domains, without an analyser. Each side of the image corresponds to 256 μm. The applied d.c. voltage values are (*a*) 0.028, (*b*) 0.500, (*c*) 2.330, (*d*) 2.870, (*e*) 3.144, (*f*) 3.410, (*g*) 4.220, (*h*) 5.590, (*i*) 6.670, and (*j*) 7.770 V.

with MBBA, was with symmetric weak–weak anchoring achieved by soap treatment of both electrodes. The electro-optical behaviour of BMAOB was studied in a wedge-shaped cell consisting of two conductive ITO coated glass plates, one rubbed with a diamond paste, the other treated with soap. We used only one Mylar spacer for this cell with a thickness of 25 μm. The cell was 50 mm long; the wedge angle was measured to be 0.026°. This small value indicates a negligible inhomogeneity of the electric field along the long side of the cell (this was confirmed in the experiment). The thickness of the MBBA cells was 12 or 50 μm. Other cells with a varied MBBA orientation were also prepared and studied. They were mentioned previously in the paragraph concerning the comparison of injection-induced domains and flexo-dielectric walls. As noted, all experimental observations were performed at room temperature.

5. Experimental results: optical observations

The first MBBA cell studied was 12 μm thick and weakly anchored. This cell was studied under d.c. voltage excitation with the procedure described above. Here we show only the images important for an understanding of flexo-dielectric walls; as noted, these domains arise in the cathode region. The sample was placed on the stage of the microscope in such a manner that the negative (−) of the voltage source was connected to the upper glass plate near the observer. The positive (+) of the voltage source was connected to the bottom glass plate. The first image of the liquid crystal layer is shown in figure 8 (*a*). The photomicrograph is taken from a picture made by a laser printer at a d.c. voltage of 0.028 V. Focusing in the depth of the liquid crystal layer shows that there are no deformations or domains inside the cell. The photomicrograph shown in figure 8 (*b*) is taken from an image made by a laser printer with the focusing in the depth of the cell, close to the cathode. The applied voltage is 0.5 V, with the polarizer perpendicular to the initial orientation of the director, i.e. perpendicular to the observed longitudinal domain patterns; no analyser was used. It can be seen that periodic deformations of the director exist at a very low voltage. In effect, these deformations began at around 0.3 V. The observed periodic deformations of the director at such a low d.c. voltage are the first reported in the literature. They could be observed due to the sensitivity of the shadowgraph technique.

These initial periodic deformations of the liquid crystal determine the flexo-dielectric walls developed later at higher voltages. This is illustrated in figures 8 (*c–h*) taken at a d.c. voltage of 2.330, 2.870, 3.144, 3.410, 4.220 and 5.590 V, respectively. One can see that adjacent domains meet at inverse walls intersecting the glass plate with surface disclinations. A new instability, perpendicular to the flexo-dielectric walls, arises at a d.c. voltage of 6.67 V; this new instability is shown in figure 8 (*i*). The development of this instability and its interaction with the longitudinal flexo-dielectric walls is shown in figure 8 (*j*) at a d.c. voltage of 7.770 V. A similar instability has been reported in previous papers [1, 2] and has been interpreted by one of the authors of this paper (H.P.H.) as the hydrodynamic domains observed by Williams. On the other hand, such an instability has been interpreted by other authors as the static flexoelectric instability of Vistin' *et al.* [33, 34]. We show a part of their picture in figure 9. A comparison of figures 8 (*j*) and 9 shows a great similarity between these two images. Without further study, however, it is difficult to clarify the origin of these domains.

The greater part of our study was made with images extracted from videotape. The rubbing-induced domains [37] and longitudinal flexo-dielectric walls are shown in figures 10 (*a*) and 10 (*b*), obtained at a d.c. voltage of 2.71 and 4.36 V, respectively. The MBBA nematic cell had a thickness of 50 μm and asymmetric strong–weak anchoring. The larger domains appear at the soap-treated cathode. At a voltage below 4 V the domains are static while at higher voltages they are electro-hydrodynamic (see the Fourier analysis in the next section). It should be noted that the new instability does not appear in such thick cells; compare figures 8 (*j*), 9 and 10 (*b*). Finally, flexo-dielectric walls appear above the rubbing-induced domains [37] and replace them in the region near the cathode for an MBBA nematic layer with a thickness of 12 μm and weak anchoring, as shown in figures 11 (*a–c*) for a d.c. voltage of 1.18, 3.014 and 5.32 V, respectively. There are, however, examples where the initial rubbing-induced domains have a smaller period, and a separation between these two types of domains still exists. This is shown in figures 12 (*a*) and 12 (*b*). Evidently these images have been made with different focusing of the microscope: at the electrode and in the depth of the liquid crystal layer These two images are important since they show that flexo-dielectric walls disturb rubbing-induced domains only in the regions where the walls meet the glass plate. This process can be caused by surface or bulk disclinations [85–87, 90, 91].

We have also investigated BMAOB, a liquid crystal displaying strong flexoelectric properties. For example, Barnik *et al.* [29, 35] observed the flexoelectric domains of Vistin' *et al.* in thin BMAOB cells. Surprisingly we have obtained new experimental results that were not observed with the other liquid crystals already studied [1–5]. We studied flexo-dielectric walls in a wedge-shaped cell with asymmetrical strong–weak anchoring

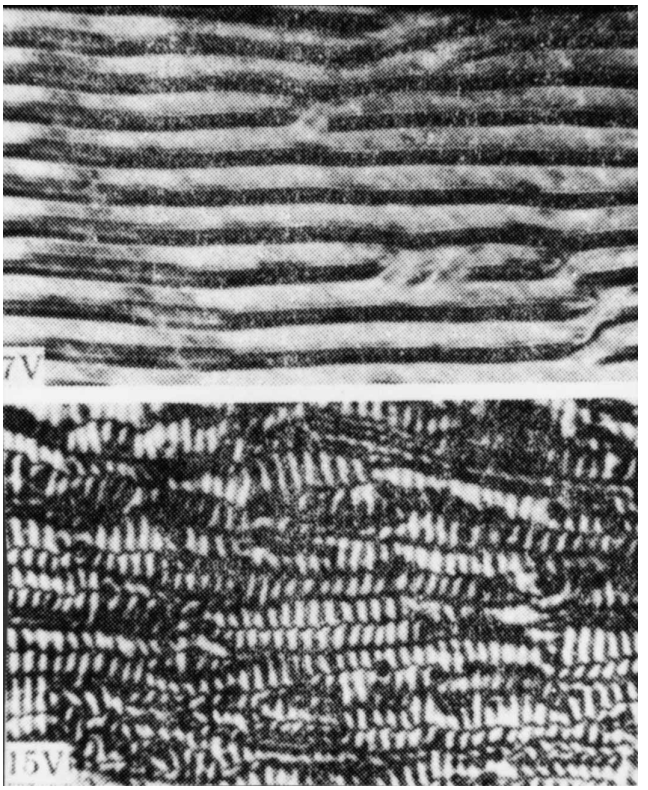

Figure 9. A microphotograph from [34] showing the simultaneous existence of longitudinal domains aligned along the long side of the picture and the flexoelectric domains of Vistin' *et al.* and Pikin *et al.* [25–33] (according to the authors of [34]) aligned in the perpendicular direction. The liquid crystal studied was MBBA with a thickness of 20 μm. The applied voltage is shown on the image (with permission of the Editors of the Bulgarian Journal of Physics).

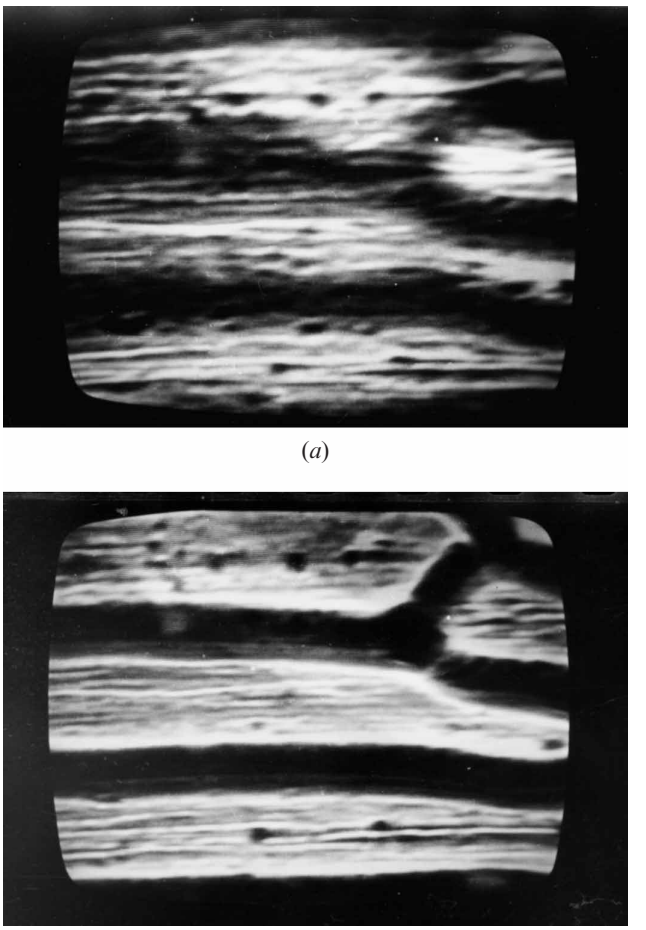

(*a*)

(*b*)

Figure 10. Rubbing-induced domains [37] and longitudinal domains (flexo-dielectric walls) in an MBBA nematic layer of thickness 50 μm and with asymmetric strong–weak anchoring. The polarizer is perpendicular to the domains, without analyser. The long side of the image corresponds to 384 μm; the images were taken from a TV screen. The applied d.c. voltage values are (*a*) 2.71 and (*b*) 4.36 V.

of the BMAOB and appropriate excitation by a d.c. voltage. The flexo-dielectric walls appeared at about 3 V when the negative (−) of the d.c. voltage source was connected to the soap-treated electrode. The domains, however, were hardly visible in crossed polarizers. This observation shows that the azimuthal ϕ-deformation is small. Indeed, rotation of the polarizer to an angle of several degrees led to the observation of black and slightly bright stripes or bands divided by black lines (the polarizer was perpendicular to the initial orientation of the liquid crystal). The domains were more discernible, however, at higher voltage with uncrossed polarizers and in monochromatic light. Figure 13 (*a*) shows the form of these domains when the analyser is rotated at an angle of 27°; the applied d.c. voltage was 5 V. These domains can be easily removed by the application of an additional a.c. voltage of 7 V at 1 kHz, above the cut-off for the charge relaxation of the space charges. The result of the application of the d.c. and a.c. voltages is shown in figure 13 (*b*).

The first new result was observed on raising the voltage, leading to undulations of the domains as shown in figure 14, an observation rarely seen with other liquid crystals showing flexo-dielectric walls. The second new result was obtained when the positive (+) of the d.c. voltage source was connected to the soap-treated electrode. The domains appeared again, this time at a slightly higher voltage (see figure 15). The domains appeared at 5 V, in the form shown in figure 15, which represents a d.c. voltage of 6 V. Again they could be removed with an additionally applied a.c. voltage of 7.5 V with frequency 1 kHz. A

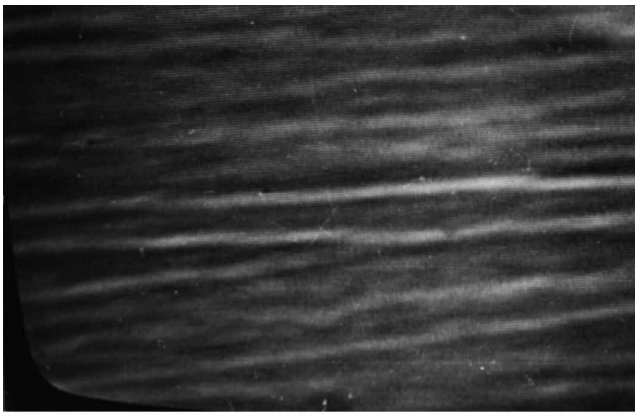

(*a*)

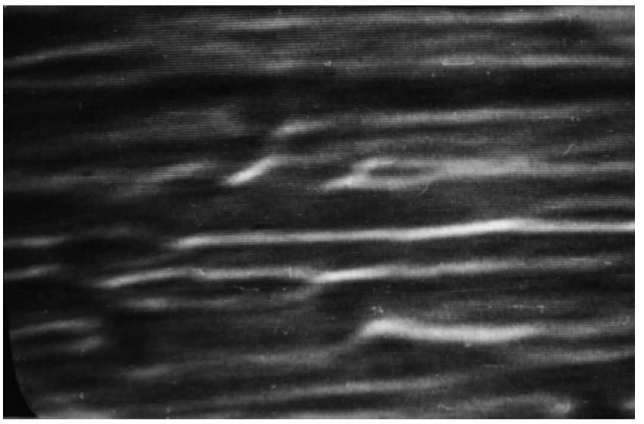

(*b*)

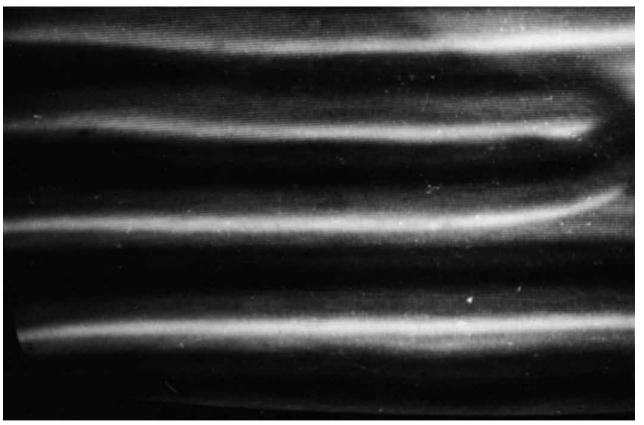

(*c*)

Figure 11. Rubbing-induced domains [37] and longitudinal domains (flexo-dielectric walls) in an MBBA nematic layer of thickness 12 μm and with weak symmetric anchoring at both electrodes. The polarizer is perpendicular to the domains, without analyser. The long side of the image corresponds to 256 μm. The images were taken from a TV screen. The applied voltage values are (*a*) 1.18, (*b*) 3.014, and (*c*) 5.32 V.

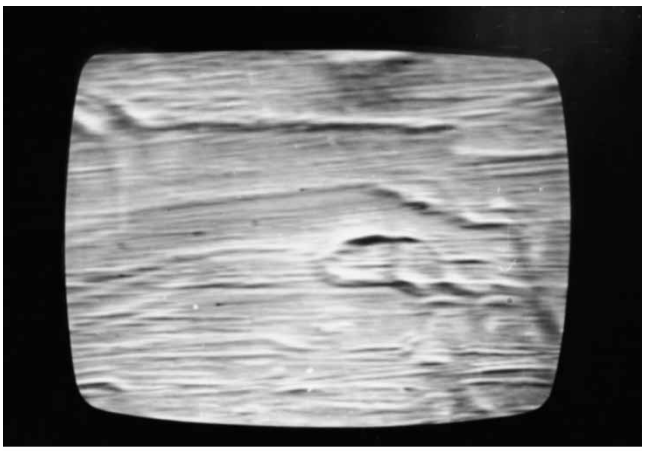

(*a*)

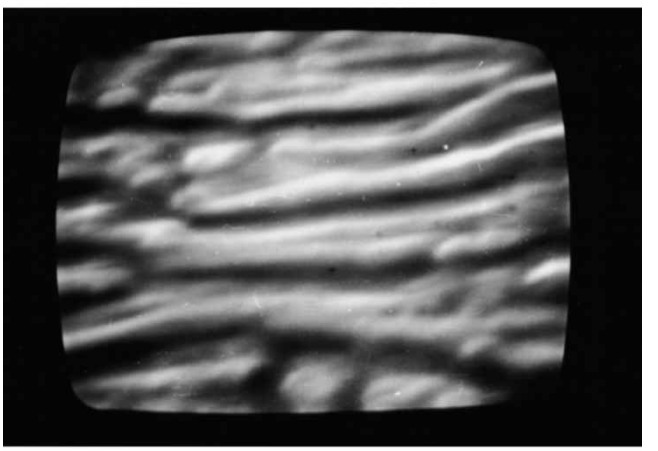

(*b*)

Figure 12. Rubbing-induced domains [37] and longitudinal domains (flexo-dielectric walls) in an MBBA nematic layer of thickness 12 μm and weak symmetric anchoring at both electrodes. The polarizer is perpendicular to the domains, without analyser. The long side of the image corresponds to 384 μm. The images were taken from a TV screen: (*a*) focusing of the polarizing microscope is on the cathode, (*b*) focusing is below the cathode, in the depth of the liquid crystal layer.

comparison of figures 13 (*a*) and 15 show that the domains are very similar and are evidently formed by the same causes.

The third, and perhaps the most important, new result was observed during the application of the d.c. voltage, independent of polarity. The flexo-dielectric walls do not appear in the thinnest part of the wedge-like cell; one example is shown in figure 16. We note that such experimental observations are absent in previous works devoted to the study of flexo-dielectric walls [1–5]. Furthermore, this thickness was unchanged at the increase of the applied d.c. voltage. On reversing the polarity, however, the flexo-dielectric walls

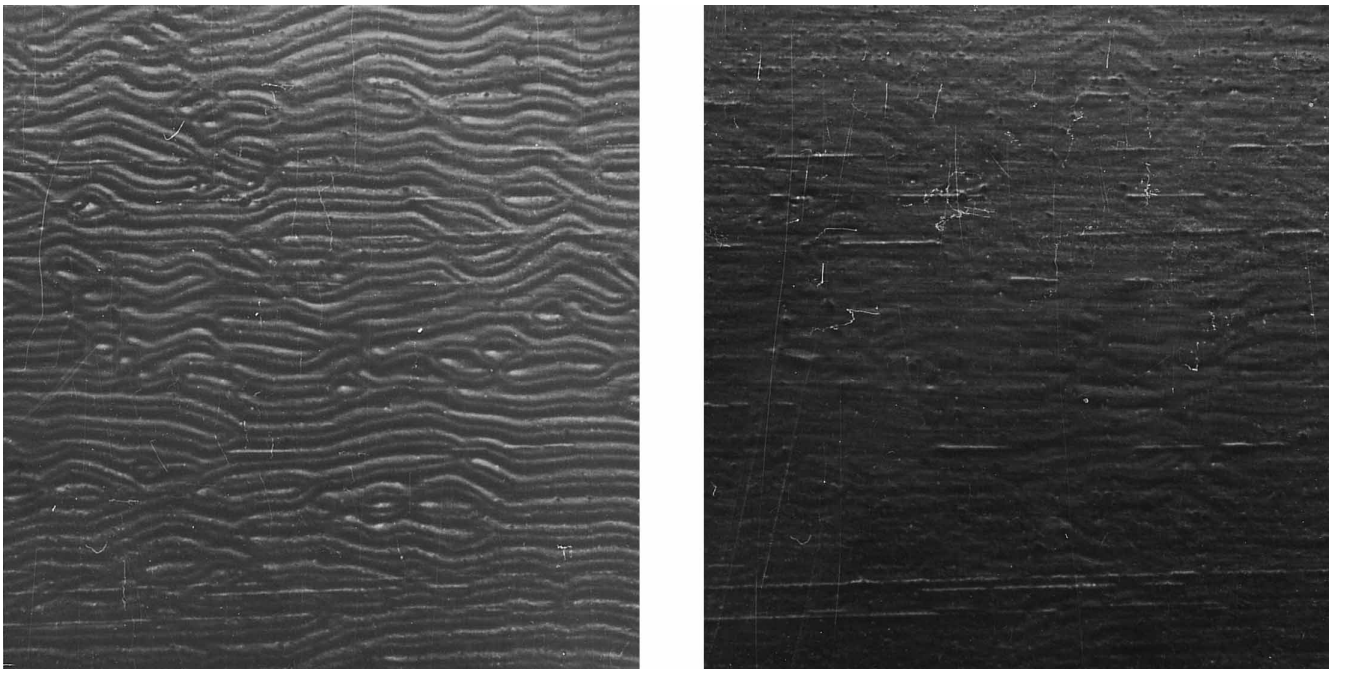

(*a*) (*b*)

Figure 13. Flexo-dielectric walls in the nematic BMAOB excited by a d.c. voltage or by d.c. and a.c. voltages. (*a*) Longitudinal flexo-dielectric walls in a wedge-shaped cell. The thickness in the domain region is 10.9 μm, A 27° $\mathbf{n}_0$ 90° P. The liquid crystal has asymmetric strong–weak anchoring. The applied d.c. voltage has amplitude 5 V; the negative (−) of the voltage source is connected to the soap-treated electrode. Each side of the image corresponds to 820 μm. (*b*) The flexo-dielectric walls are erased by an additionally applied a.c. voltage of 7 V with frequency 1 kHz.

penetrate into the thinner part of the cell, which is followed by their gradual disappearance. Moreover, in this liquid crystal we observed the flexoelectric domains of Vistin' *et al.* in the thinnest part of the cell. We

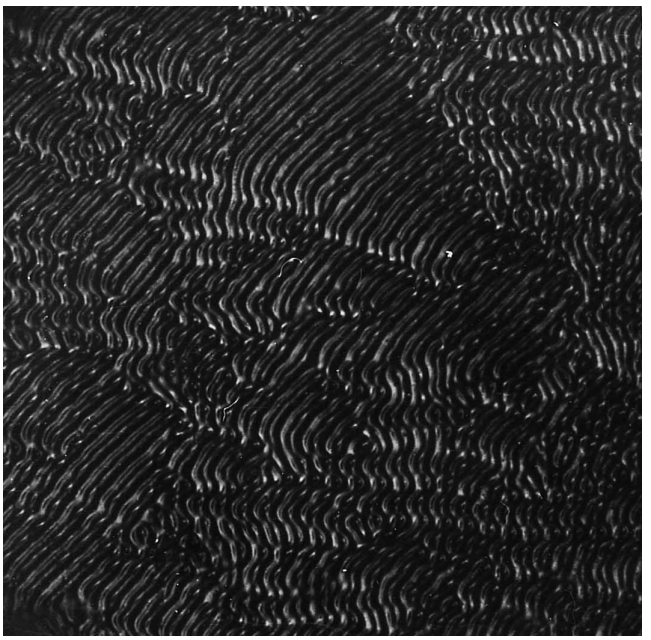

Figure 14. Undulations of the domains shown in figure 13 (*a*) under a d.c. voltage of 7 V.

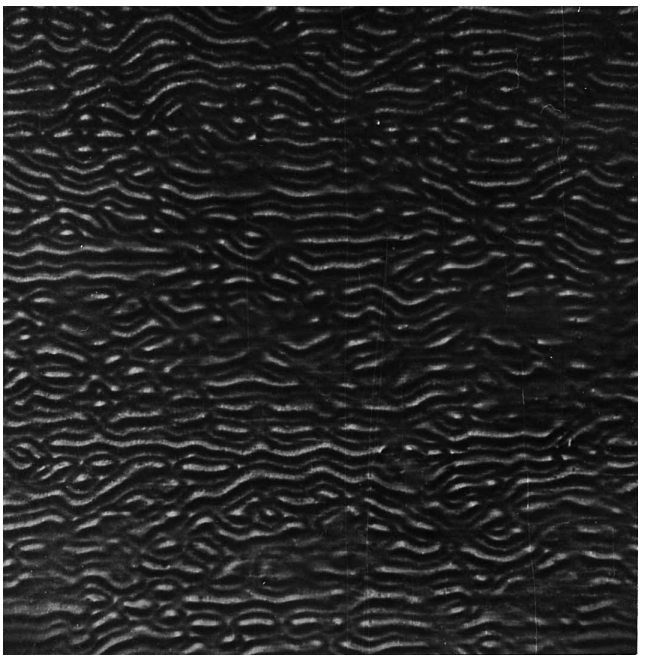

Figure 15. Longitudinal flexo-dielectric walls in a wedge-shaped cell with the nematic BMAOB. The thickness in the domain region is 10.9 μm, A 27° $\mathbf{n}_0$ 90° P. The liquid crystal has asymmetric strong–weak anchoring. The applied d.c. voltage has amplitude 6 V; the positive (+) of the voltage source is connected to the soap-treated electrode. Each side of the image corresponds to 820 μm.

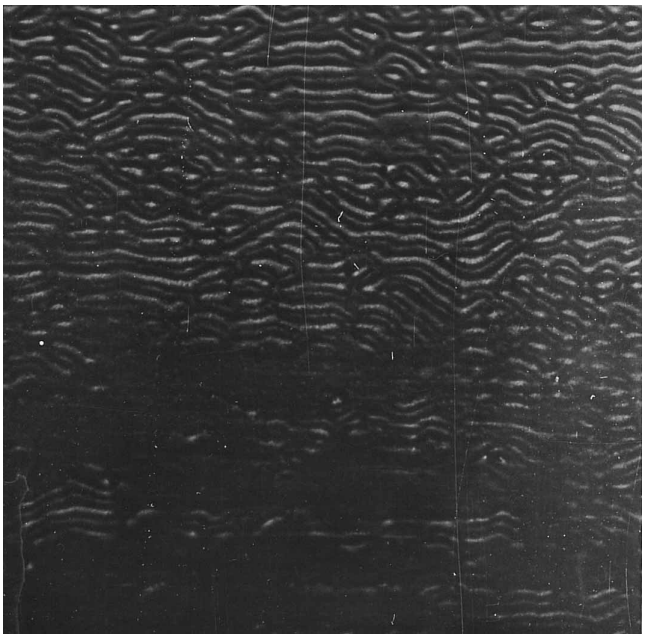

Figure 16. The domains from figure 15 observed at a thickness of 9.5 μm, and their disappearance in the thinner part of the cell.

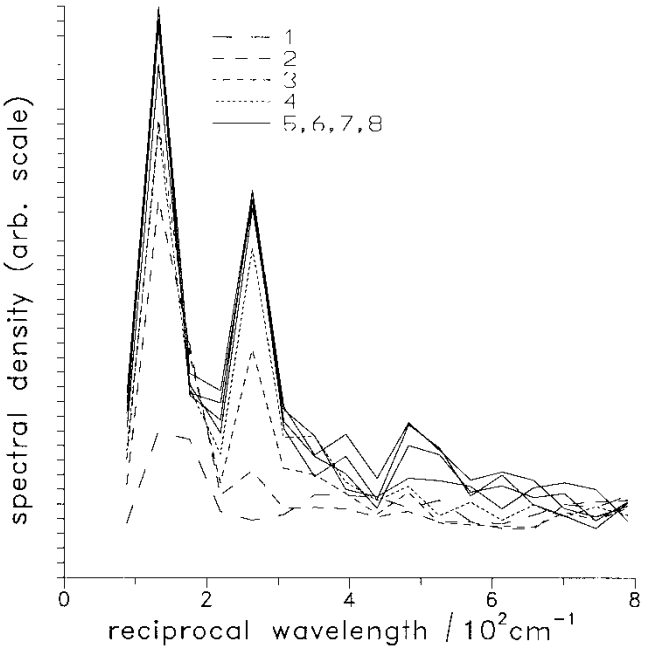

Figure 17. The spectral density (in arbitrary units) of the transmitted polarized light through the MBBA nematic **K** cell (see the text concerning Fourier analysis results) at room temperature as a function of the inverse period (in cm^{-1}) of the flexo-dielectric walls. See text for d.c. voltage conditions.

have never observed the simultaneous existence of the flexoelectric domains of Visin' *et al.* and flexo-dielectric walls.

6. Fourier analysis (FA) results

The following images were stored in the computer: (a) images from figure 8 designated as **F** cells; (b) images similar to those shown in figure 10, at various d.c. voltages extracted from videotape designated as **K** cells; (c) images similar to those shown in figures 11 and 12, at various d.c. voltages also extracted from the videotape and designated as **M** cells.

The Fourier analysis processing of images from cells **F**, **K** and **M** are shown and discussed in this part of the paper. Image processing details were given in § 4. The FA curves of the images obtained with **K** cells (50 μm thick nematic MBBA layer with asymmetric strong–weak anchoring) under the application of a d.c. voltage with various amplitudes are shown in figure 17. Curve 1 corresponds to a d.c. voltage of 1.18 V. Curves 2–8 correspond to voltages of 2.99, 3.54, 4.09, 4.63, 5.18, 5.75 and 6.28 V, respectively. As noted above, similar pictures are shown in figures 10 (*a*) and 10 (*b*) (see also [37]), at d.c. voltages of 2.71 and 4.36 V, respectively. It is clear from these curves that the domain period is fixed. Consequently, these domains represent flexo-dielectric walls. It is also clear that above a d.c. voltage of 4.63 V the domains become electro-hydrodynamic. The average period of the domains was measured to be around 2*d* (92 μm), where *d* is the thickness of the liquid crystal layer. The form of the curves shown in figure 17 indicate that the optical image of the flexo-dielectric walls contains first, second and fourth harmonics. Additionally, we have investigated the appearance and development of these walls along one pre-selected line including, as noted, 512 pixels. The FA results along an arbitrarily chosen line, perpendicular to the domains, are shown in figures 18 (*a–c*) for an applied d.c. voltage of 1.18 V (no domains), 4.09 V (development of the domains) and 6.28 V (transformation into electro-hydrodynamic domains). A comparison of figures 18 (*b*) and 18 (*c*) reveals a slight translation of the domains by several microns, probably due to hydrodynamic effects.

The FA curves of the domains obtained with **M** cells (12 μm thick MBBA nematic layer with symmetric weak anchoring and a reverse tilt at the boundaries, giving nearly planar orientation of the layer) are shown in figure 19. Curve by 1 corresponds to a d.c. voltage of 1.18 V; curves 2–8 correspond to d.c. voltages of 2.99, 3.54, 4.09, 4.64, 5.18, 5.75 and 6.28 V, respectively. Careful study of these curves shows that the liquid crystal deformations arise from a nearly planar and oriented nematic layer. The period of the domains slightly decreases with increase of the voltage and changes from 31 μm at the threshold to 22 μm at a

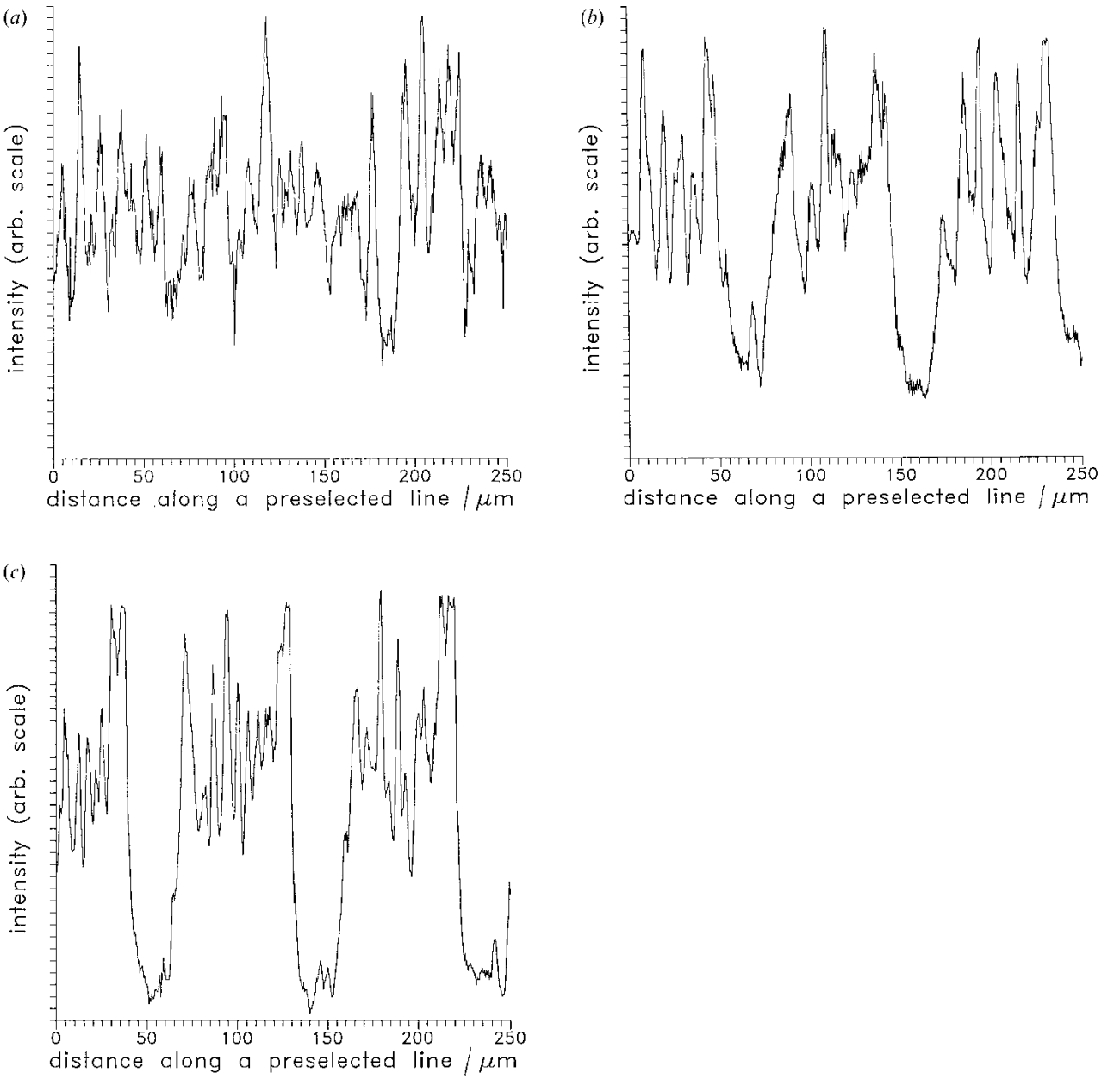

Figure 18. The spectral density (in arbitrary units) of the transmitted polarized light through the MBBA nematic **K** cell (see the text, concerning the Fourier analysis results) at room temperature, as a function of the distance along one arbitrarily preselected line (in micrometers) perpendicular to the flexo-dielectric walls, for the following amplitudes of the d.c. voltage applied across the cell: (*a*) 1.18, (*b*) 4.09 and (*c*) 6.28 V.

voltage of 5.18 V (curve 6). At d.c. voltages of 5.18, 5.75 and 6.28 V the period of the domains is the same. Evidently in this voltage range the initially static flexo-dielectric walls are transformed into hydrodynamic domains. On the other hand, comparison of the curves shown in figures 17 and 19 shows that the domains obtained in symmetrically weakly anchored MBBA nematic layers are more symmetrical than to those obtained in asymmetrical strong–weak anchored MBBA nematic layers. In our opinion, they contain first, second and third harmonics.

Finally we show the FA curves for **F** cells (see figure 20). A comparison of the curves from figures 17, 19, and 20 shows that the images obtained from the videotape are much better than those made by the laser printer, as expected. Nevertheless, the curves 1, 2, 3 and 4 in figure 20, corresponding to d.c. voltages of 0.028, 0.300, 2.600 and 3.144 V, respectively, clearly

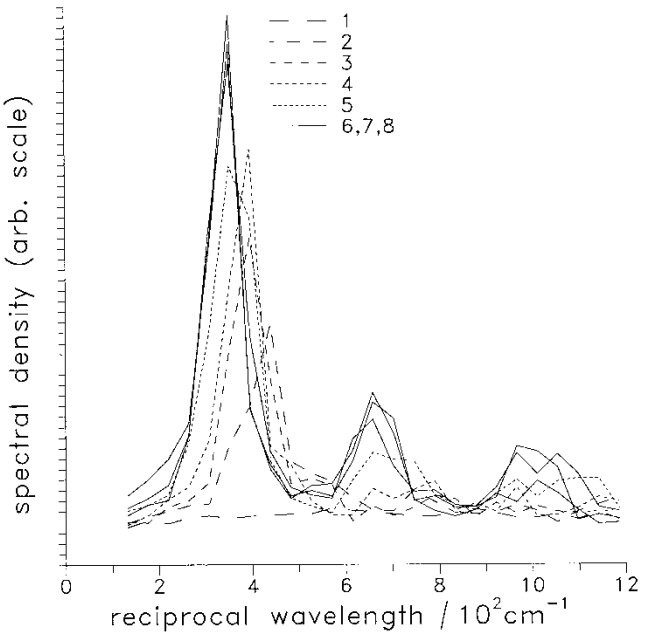

Figure 19. The spectral density (in arbitrary units) of the transmitted polarized light through the MBBA nematic **M** cell (see the text, concerning the Fourier analysis results) at room temperature as a function of the inverse period (in cm^{-1}) of the flexo-dielectric walls. See text for d.c. voltage conditions.

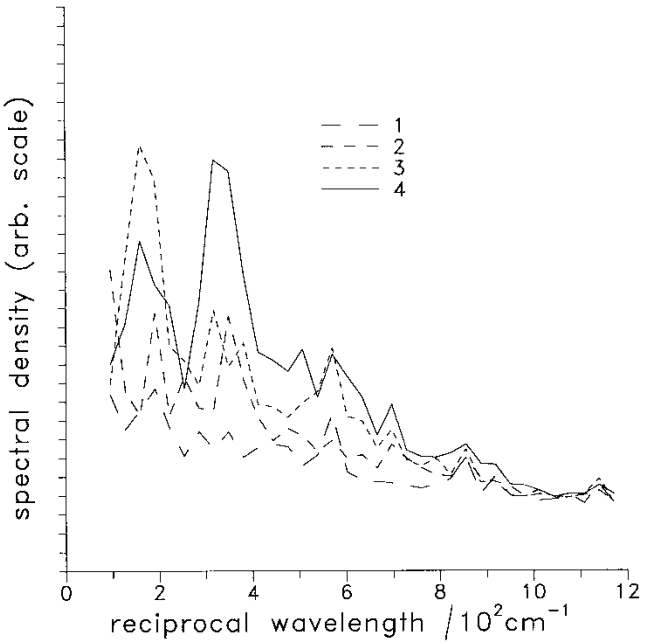

Figure 20. The spectral density (in arbitrary units) of the transmitted polarized light through the MBBA nematic **F** cell (see the text, concerning the Fourier analysis results) at room temperature as a function of the inverse period (in cm^{-1}) of the flexo-dielectric walls. See text for d.c. voltage details.

demonstrate that the domains develop on the initial deformation with the largest period. Furthermore, the largest changes are at a voltage of 3.144 V. This probably coincides with the beginning of the Fréedericksz transition. Figures 17 and 20 clearly show that flexo-dielectric walls develop on the largest deformation. There are, however, examples where the appearance of the domains disturbs either the already existing initial deformations in the form of rubbing-induced domains [37] (figure 11), or are developed from well aligned reverse-tilted layers (figure 19). In effect, the initial tilt of the nematic layer accompanied by the initial azimuthal splay deformation which is developed along the OY axis, and the existence of a strong gradient flexoelectric effect along the OZ axis, combined with the stabilizing action of the dielectric torque on the polar θ-deformations, are crucial for the appearance of flexo-dielectric walls. This will be discussed below.

7. Comment on possible causes of the formation of flexo-dielectric walls: preliminary theoretical considerations, a proposal of a model and experimental evidence connected with this model

The experimental results and observations concerning the appearance and development of flexo-dielectric walls in various nematics with a small negative dielectric anisotropy (MBBA [1–5] this paper, the liquid crystal 440 and PAA [2] and, finally, the liquid crystal BMAOB this paper) clearly show that they are a manifestation of the so-called gradient flexoelectric effect [19, 20], known in the literature as a quadrupolar flexoelectric effect discovered and investigated by Prost and Marcerou [92, 93]; some aspects of the quadrupolar flexoeffect have been also discussed by Goossens [94]. Flexo-dielectric walls usually appear in the cathode region and are apparently connected with the formation of space charge layers sustained by the current. These walls can be formed also (this paper) under a very low d.c. voltage (below 1 V), evidently connected with the formation of double electric layers. In some cases, e.g. BMAOB, the walls appear at either the cathode or the anode. Indeed, the study of the electrochemical behaviour of the nematic BMAOB [47, 95], demonstrates the existence of injection from either the cathode or the anode. This fact, combined with the strong flexoelectric properties of this liquid crystal, explains the appearance of flexo-dielectric walls at either the cathode or the anode. Here we should mention, however, that the existence of double injection leads to difficulties in the formation of flexo-dielectric walls because it greatly enlarges the thickness of the space charge layers from 1 to 50 μm for the case of a nematic, similar to MBBA [44]. Our experimental results concerning the flexoelectric behaviour of BMAOB

demonstrate that there is no relation between the flexo-dielectric walls discovered and studied by Hinov *et al.* [1–5], this paper, and the flexoelectric domains of Vistin' *et al.* and Pikin *et al.* [25–34].

The visual form of flexo-dielectric walls is very similar to that of other domains obtained in lyotropic nematics [96, 97], nematic side group polysiloxane [98] (pattern formation at the splay Fréedericksz transition), and to banded textures induced by an electric field in polymeric liquid crystalline solution [99]. All these domain patterns can be explained by the formation of a periodic instability of the dynamics accompanied relaxation of the Fréedericksz transition [13]. It is important to note that all these examples are characterized by a sudden change of the initial distribution of the liquid crystal director, for example by the application of an electric field [99], a magnetic field [13] or other forces such as shearing. These sudden changes prevent the liquid crystal from relaxing the strains by clockwise or counter-clockwise rotation of the director in adjacent bands [99]. It is more difficult, however, to explain the formation of flexo-dielectric walls by the sudden change in the orientation of the liquid crystal, or by a sudden change in direction of the applied d.c. voltage, since such changes have not been observed and have not been generated experimentally. Indeed, in some papers calculations show that at some circumstances near the injecting electrode there is a region where the electric field can change its sign [100]. We do not believe, however, that this is the only cause of the development of flexo-dielectric walls. From all experimental results obtained hitherto, it is known only that the formation of flexo-dielectric walls is connected with the formation of space charge layers near the electrodes. We now comment on the possible causes leading to the formation of flexo-dielectric walls including preliminary theoretical considerations and the proposal of a new model supported by experimental evidence obtained in this paper and elsewhere.

As noted, we believe that the appearance of flexo-dielectric walls is connected with the quadrupolar flexoelectric effect, evidenced in nematics with flexoelectric properties placed in a gradient electric field. The possible distribution of the director **n** in the space can be represented by the following vector equation [8, 101, 102]:

$$\mathbf{n}\times\mathbf{h}_{\mathrm{f}}=0$$
$$\mathbf{h}_{\mathrm{f}}=K\Delta\mathbf{n}-(e_{1z}+e_{3x})(\mathbf{n}.\mathrm{grad})\mathbf{E}-\frac{\Delta\varepsilon}{4\pi}(\mathbf{E}.\mathbf{n})\mathbf{n} \tag{4}$$

where $\mathbf{h}_{\mathrm{f}}$ is the molecular vector field introduced for the first time in liquid crystal theory by de Gennes [8] (we have neglected the flexoelectric effects arising in a homogeneous electric field and have assumed isotropic elasticity: $K_{11}=K_{22}=K_{33}=K$).The vector equation (4) leads to the following two differential equations for the director components n_y and n_z ($n_x=\mathrm{const}$):

$$(h_{\mathrm{f}})_y=K\left(\frac{\partial^2 n_y}{\partial y^2}+\frac{\partial^2 n_y}{\partial z^2}\right)-(e_{1z}+e_{3x})\left(\frac{\partial E_y}{\partial y}n_y+\frac{\partial E_y}{\partial z}n_z\right)-\frac{\Delta\varepsilon}{4\pi}(E_y n_y+E_z n_z)E_y=0 \tag{5a}$$

$$(h_{\mathrm{f}})_z=K\left(\frac{\partial^2 n_z}{\partial y^2}+\frac{\partial^2 n_z}{\partial z^2}\right)-(e_{1z}+e_{3x})\left(\frac{\partial E_z}{\partial y}n_y+\frac{\partial E_z}{\partial z}n_z\right)-\frac{\Delta\varepsilon}{4\pi}(E_y n_y+E_z n_z)E_z=0 \tag{5b}$$

where $(h_{\mathrm{f}})_y$ and $(h_{\mathrm{f}})_z$ are the torques which rotate the director along the y and z directions. Additionally, it is clear [103] that the following equality:

$$\frac{\partial E_y}{\partial z}=\frac{\partial E_z}{\partial y} \tag{6}$$

is valid since rot $\mathbf{E}=0$ and the following relations are performed:

$$E_z=E_0+E_{z_1}(z,y),\ E_{z_1}<<E_0$$
$$E_y=E_y(z,y),\ E_y<<E_0. \tag{7}$$

The form of the equations (5*a*) and (5*b*) shows that a solution can be found for the director components n_y and n_z even when the Frank elasticity is ignored. In our opinion this is not a surprising result since such solutions can be found in the electro-hydrodynamic theory of liquid crystals [8] or in the ionic behaviour [8, 104]. From experiment we know that flexo-dielectric walls arise from tilted layers with one exception: the cross-like domains which appear in a homeotropic nematic layer. Since the rotation of the director starts from one tilt position, it can be performed in two opposite directions. This mechanism leads to the development of the wall. Equations (5) show also that development of the walls is impossible for the particular case when the dielectric anisotropy of the nematic vanishes. In other words, the walls developed are flexo-dielectric in their nature. At this point two questions can be posed. The first is connected with the creation of the non-homogeneous electric field along Z and Y; the second concerns the behaviour of flexo-dielectric walls above the threshold. As far as the non-homogeneous electric field due to the accumulation of ions along the OZ and OY directions is concerned, following well known differential equations may be considered.

Poisson equation

$$\nabla.\mathbf{D}=4\pi q \tag{8}$$

where $D_i=\varepsilon_{ij}E_j+4\pi P_i$, ε_{ij} is the dielectric tensor, representing the dielectric properties of the nematic

and P_i is the flexoelectric polarization:

$$\mathbf{P} = e_{1z}\,\mathrm{div}\,\mathbf{n} + e_{3x}(\mathbf{n}\times\mathrm{rot}\,\mathbf{n}). \tag{9}$$

Charge conservation equation

$$\frac{\partial q}{\partial t} + \nabla.\mathbf{J} = 0 \tag{10}$$

where the current **J** in general has three components, ohmic, charge-injection and diffusional:

$$J_i = J_{\sigma_i} + J_{\mu_i} + J_{d_i} \tag{11}$$

where

$$\begin{aligned} J_{\sigma_i} &= \sigma_{ij}E_j \\ J_{\mu_i} &= q^{\alpha}\mu^{\alpha}_{ij}E_j \\ J_{d_i} &= -D^{\alpha}_{ij}q^{\alpha}_{,j} \end{aligned} \tag{12}$$

and α represents the different ions in the liquid crystal cells.

It is well known that diffusion is important for low electric fields when the drift and diffusion components of the current (along Z or along Y) are comparable [44, 105, 106]. According to Schilling and Schachter [106] diffusion is important for a voltage in the region of $3D/\mu$, which for the case of the nematic diffusion constant D [107] and the mean mobility of the ions [108] is in the region of 0.3 V (let us recall that we have observed the formation of flexo-dielectric walls at such a low d.c. voltage). According to Turnbull, however, diffusion can also be important at higher voltages [44]. This occurs at the edges of space charge layers, which according to Turnbull have a thickness of 1 μm for unipolar injection and 50 μm for bipolar injection for sufficiently thick nematic layers. The thickness of the space charge layer at the injecting electrode has been estimated by Turnbull on the basis of the following formula (ion diffusion was neglected):

$$L_{\mathrm{I}} \propto \frac{J_z\varepsilon\varepsilon_0}{\sigma^2\mu} \tag{13}$$

where J_z is the component of the current along the Z axis, ε is the dielectric constant of the liquid crystal, ε_0 is the dielectric constant of vacuum, σ is the conductivity of the liquid crystal and μ is the charge carrier mobility.

Diffusion should be taken into account at the edges of the space charge layer along a thickness proportional to kT/eE, where k is the Boltzman constant, T is the absolute temperature, e is the electronic charge and E is the value of the applied electric field. The characteristic length estimated by Turnbull [44] is about 0.1 μm for a d.c. voltage in the range 3–5 V. In our opinion, flexo-dielectric walls appear mainly in this region. For a purely ohmic material, the non-uniform electric field should be within one characteristic length similar to the Debye characteristic length, estimated by Dubois-Violette [109] to be:

$$L_{\mathrm{D}} \propto (\tau D)^{\frac{1}{2}} = \left(\frac{\varepsilon\varepsilon_0 D}{\sigma}\right)^{\frac{1}{2}} \tag{14}$$

where D is the diffusion constant, typically in the region of $10^{-7}\,\mathrm{cm^2\,s^{-1}}$ [107] and σ is the ohmic conductivity, typically in the range 10^{-8}–$10^{-11}\,\Omega^{-1}\,\mathrm{cm^{-1}}$, $\varepsilon = 5$, $\varepsilon_0 = 8.85\times10^{-14}\,\mathrm{F\,cm^{-1}}$. This thickness should be in the range 10^{-6}–10^{-5} cm, an anticipated value for a conducting nematic. Zahn [110] has considered injection in one material possessing an ohmic conductivity; his general conclusions, important for our model, is that injected ions are accumulated near the injecting electrode in the range (0.2–0.3)d, where d is the thickness of the cells under study, whereas space charges are neutralized in the rest of the cell with time constant $\tau = \varepsilon\varepsilon_0/\sigma$.

Another important problem connected with equations (5 *a*) and (5 *b*) is the existence of the E_y component of the electric field. Several mechanisms lead to the creation of this component. The first one is the existence of $n_y(y)$ fluctuation, which can be amplified by the Carr–Helfrich–Pikin mechanism [9–12]. Evidently in this mechanism the anisotropy of either the conductivity [9–12], or of both the conductivity and diffusivity, should be included (the role of diffusion is mentioned in a number of papers devoted either to the injection phenomenon [100, 106] or to the process of formation of injection domains [111, 112]). The E_y component can also be created by flexoelectric charge density when both the conductivity and diffusivity are isotropic. For example, Lange *et al.* have considered this problem for the oblique rolls in nematic liquid crystals, including flexoelectricity [113]. The third way to create an E_y component is to prepare a grooved electrode [37]; furthermore, the existence of defects (and certainly of grooves) in the dielectric layer covering the electrode, or in the conducting glass plate, can also lead to a strong non-homogeneous electric field leading to the observation of the gradient flexoelectric effect [114, 115]. In addition, the transversal component of the current along y is important; this leads to the accumulation of space charges in this direction and to the creation of the transverse component of the electric field.

On the basis of all the experimental observations concerning flexo-dielectric walls and the preliminary theoretical considerations presented above, and on the basis of the results and mechanisms obtained and proposed by others, we have created a new model which qualitatively explains the appearance and development of flexo-dielectric walls. This model is schematically

shown in figures 21 (*a*) and 22 (*a*) and represents the rotation of the director **n** around the *OX* axis ($n_x = const$) and the distribution of the space charges for both unipolar or bipolar injection. We show the maximum and minimum for negative charges in the case of unipolar injection from the cathode, and the maximas for positive and negative charges in the case of bipolar injection. Since flexoelectric deformations arise in the form of walls, we elaborate this model further, taking into account some results obtained by Carr [116, 117]. Flexoelectric torques could be removed only by splay azimuthal realignments of the director. They should redisribute the injected space charges, arranging them in vertical planes. This is done by the Carr–Helfrich–Pikin-flexoelectric mechanisms [8, 9–12].

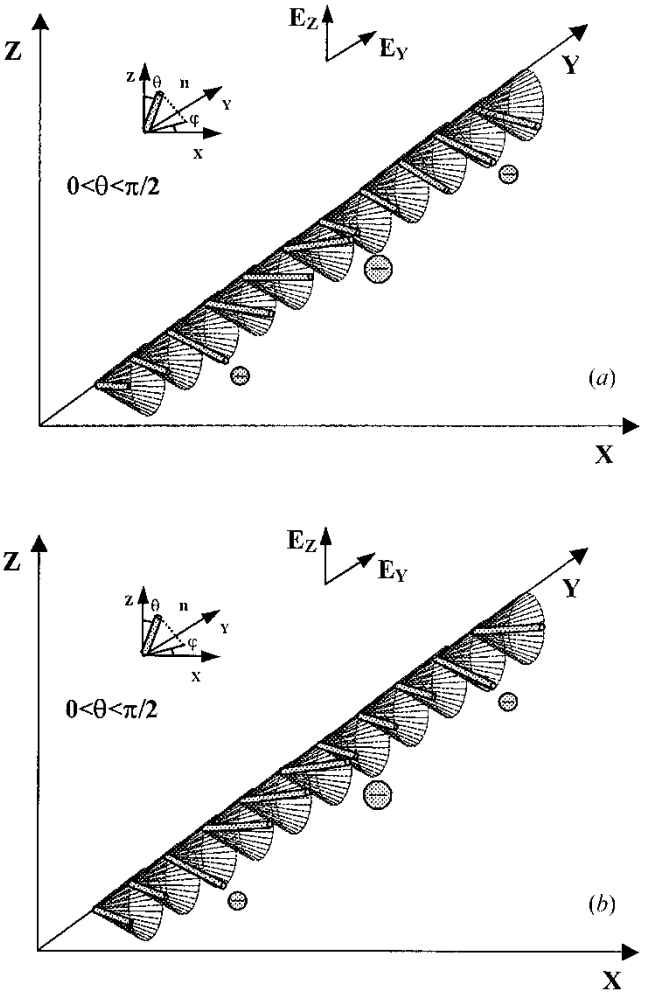

Figure 21. A schematic representation of current redistributed space charges for the case of unipolar injection for a splay deformation along the *OY* axis: (*a*) the beginning of the charge redistribution; (*b*) the final picture of the charge distribution and the zig-zag orientation of the liquid crystal inside the walls.

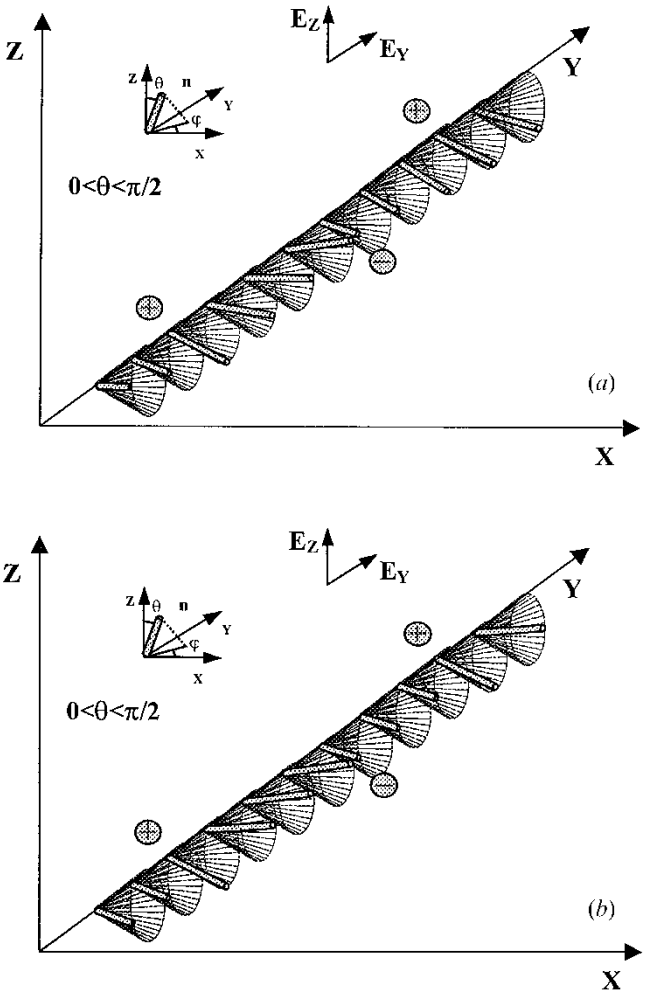

Figure 22. A schematic representation of the current redistributed space charges for the case of bipolar injection for a splay deformation along the *OY* axis: (*a*) the beginning of charge redistribution; (*b*) the final picture of the charge distribution and the zig-zag orientation of the liquid crystal inside the walls.

This new redistribution of the ions is affected not only by initial azimuthal deformations, always existing in one weakly-anchored nematic layer, but also by anisotropy of the conductivity (thin cells, high d.c. voltage) or by anisotropy of the diffusivity (thick cells, low d.c. voltage, double electric layers) of the liquid crystal.

The appearance and development of flexo-dielectric walls and their peculiar optical form show that they represent $+\phi$ and $-\phi$ bands, as in the case of the splay Fréedericksz transition [98]; this is schematically illustrated in figures 21 (*b*) and 22 (*b*). However, there are examples where flexo-dielectric walls represent θ-bands with different values of the polar deformations of the director. All the forms of the walls can be explained

by the arguments of Carr [116, 117] with the following two differences. First, the electro-hydrodynamic torques acting along the charged vertical sheets [116–118] are replaced by quadrupolar flexoelectric torques; second, equally charged planes are arranged at a distance approximately twice the thickness of the liquid crystal layer in the case of unipolar injection (this argument is not valid for a thin cell with a thickness below 10 μm, since in this case the electric forces between the charged walls are stronger). In the case of bipolar injection, the distribution of positive and negative charges in vertical sheets should be alternative; see the figures 22 (*a*) and 22 (*b*). It is well known that inside such charged walls the electric field has the following form:

$$E_y = \frac{4\pi\rho}{\varepsilon\varepsilon_0} y \tag{15}$$

where ρ is the charge density. Outside the wall the electric field can be expressed by:

$$E_y = \frac{4\pi\rho a y}{|y|} \tag{16}$$

where a is the thickness of the space charge layer.

The electric field along the Y axis is non-homogeneous inside the charged sheets and homogeneous with different signs outside them according to the formulae (15) and (16). The strong quadrupolar flexoelectric torques created by the strong non-homogeneous electric field inside the sheets, together with the wall construction of the flexo-dielectric domains terminating with surface disclinations on the electrode, counteract the electro-hydrodynamic torques. At higher voltages however, the electro-hydrodynamic torques are stronger and one observes movement of the fluid inside the domains. This occurs usually around 4–5 V. Here we should mention that the change of the space charge layer from a vertical sheet to a cylindrical form greatly complicates the problem, transforming the electric field from one-dimensional to three-dimensional. In these cases the domains are quite complex, as are the cross-like domains [2] or the π-walls (figure 4).

We now consider the solution of the differential equations (5 *a*) and (5 *b*) describing the director components n_y and n_z (the flexoeffect in a homogeneous electric field is ignored since in the experiment we observed no relationship between flexo-dielectric walls and the flexoelerctric domains of Vistin' *et al.*). In the regions of strongest deformation, where the deformational angles change their sign, one cannot ignore the Frank elasticity and the equations should be solved without approximations. Finally, we mention that the redistribution of the injected ions in vertical sheets releases stresses and leads to the final development of flexo-dielectric walls. The increase of the d.c. voltage, however, increases deformations inside the walls and this is experimentally shown by the form of the flexo-dielectric walls.

The redistribution of injected ions is effected by the dynamics in the change of the director components. They can be expressed simply by equating the left-hand sides of equations (5*a*) and (5 *b*) to $\gamma(\partial n_y/\partial t)$ and $\gamma(\partial n_z/\partial t)$, respectively [8–12]. The formation of vertical sheets of unipolar ions should lead to some asymmetry in the disposition of every pair of adjacent bands, since the charges are unequal; see figures 21 (*a*) and 21 (*b*). Such a distribution of the injected ions can exist at unipolar injection or at the formation of double electric layers. In addition, it is clear that the interaction of a more highly charged disclination, or wall with the electrode surface, should be stronger than the interaction of a less charged disclination or wall with the same electrode surface [119]. Indeed, adjacent bands in the flexo-dielectric walls were formed often at different depths of the liquid crystal layers [1–5].

Flexo-dielectric walls can be destroyed when there is overlapping of the (+) and (−) space charge layers in such a manner that they are totally compensated. This process transforms the conductivity from injection to ohmic [120]. This case was observed in our experiment with the liquid crystal BMAOB. In some places one can see only traces of flexo-dielectric walls (see figure 16). We will now discuss several important problems concerning the formation of flexo-dielectric walls.

The first problem is connected with the formation of double electric layers. The dynamic formation of double electric layers is related to the time needed for the ions to reach the electrode; this is equal to $d/2\mu E_0$, where d is the thickness of the cell, μ is the mobility of the ion and E_0 is the value of the applied electric field. The estimated value is less than 1 s for thin cells up to 100 s for thick cells; this is in agreement with our experimental results [1–5]. Furthermore, it is evident that this formula can be used also for the movement of ions inside the domains in the frame of the Carr–Helfrich–Pikin model (one should however change the value of the electric field by E_y).

The second problem concerns diffusion processes. These are important as noted above at low voltages (below 1 V), in thick cells (above 100 μm), at the edges of the inner space charge layers, at the formation of double electric layers, at the reversal of the sign of the d.c. voltage, and at the switch-off of the voltage. The change of charge with the time is proportional to $\exp(-\pi^2 Dt/d^2)$ where D is the diffusion constant, t is the time and d is the thickness of the liquid crystal layer [121]. It is well known that diffusion

processes are the slowest process in liquid crystal cells, and that they can continue for many seconds and even minutes.

The third problem relates to the value of the electric field and the sign of its gradient. Since the flexoeffect is linear, at a high electric field dielectric effects prevail while at a lower electric field flexoelectric effects prevail. Further, it is well known that the electric field is stronger and homogeneous at the collecting electrode and lower and non-homogeneous at the injecting electrode in the case of unipolar injection (for one ohmic material) [110]. In other words, at the appropriate sign of the total flexoelectric coefficient $(e_{1z}+e_{3x})$, the region at the injecting electrode is more favourable for the development of flexo-dielectric walls. In the case of double electric layers, the more favourable region for the development of flexo-dielectric walls is close to the electrode in the diffusion part of these layers. The cases of the overlapping of a double electric layer with the injection layer, and double injection, are more complex and are considered in detail by Cocco *et al.* [47] and by Turnbull [44], respectively.

The fourth problem concerns the screening of flexoelectric charges by movable free space charges in the case of walls. This problem has been discussed in several papers by Pikin *et al.* for the dislocation walls observed in the SmC* phase [122, 123]. We should note that the form of the flexo-dielectric walls in nematics and of the piezoelectric dislocation walls in SmC* is very similar. Furthermore, neither wall forms appear in pure material. Evidently the existence of free charges in the liquid crystal is important since they screen the flexoelectric charges, decrease the flexoelectric (resp. the piezoelectric) energy and stabilize the domains. This is very well explained in the papers of Pikin *et al.*

The final problem concerns the disappearance of flexo-dielectric walls on losing anchoring of the nematic at the conductive glass plates. This case is considered by Pikin for azimuthal electro-hydrodynamic instabilities [12]. According to Pikin a vanishing anchoring cannot support the initial deformations along the azimuthal angle ϕ; thus, it is impossible to amplify these initial deformations. In addition, vanishing anchoring prevents the formation of walls and surface disclinations as was observed in the case of flexo-dielectric walls [2].

In conclusion, we have performed additional experiments with the nematic MBBA, showing the formation of flexo-dielectric walls known as parallel surface-induced flexoelectric domains (PSIFED). We have used new tools for their study—the shadowgraph technique accompanied by computer processing of the more important images. We have demonstrated experimentally, for the first time, that the formation of the domains can start at the very low d.c. voltage of 0.3–0.5 V when double electric layers are formed. We have observed, for the first time, flexo-dielectric walls in the liquid crystal BMAOB in the thicker regions of a wedge-shaped nematic cell, and the flexoelectric domains of Vistin' *et al.* and Pikin *et al.*, in the thinnest part of the same wedge-shaped cell. We have never seen the overlapping of these two flexoelectric modes. It was evident that there is no relation between these two types of flexoelectric domain.

We have observed, for the first time, the interaction of rubbing-induced domains [37] known for a long time, but not studied in detail, with the flexo-dielectric walls. Our images clearly show that the flexo-dielectric walls penetrate up to the electrodes only at places where pairs of adjacent walls terminate. We propose a simple model that explains the appearance of flexo-dielectric walls and that includes the three possible causes: the formation of double electric layers, unipolar injection and bipolar injection. According to our suggestions, flexo-dielectric walls arise in one very thin layer with a thickness less than 1 μm. It is embedded into the rest of the homogeneously tilted nematic layer. The non-homogeneity of the electric field in this layer leads to strong quadrupolar flexoelectric torques rotating the director around the X axis and outside the XZ plane in two opposite directions.

In addition, anisotropic properties of the liquid crystal, including conductivity, diffusivity and the flexoelectric effect, the existence of initial tilt and initial azimuthal deformations stimulated by the weak azimuthal anchoring of the liquid crystal, all lead to redistribution of the ions and to the formation of vertical charged sheets with a higher density of ions. These ionic sheets consist of (a) some-sign charges and a different density (unipolar injection: MBBA, PAA, liquid crystal 440) or (b) of charges of both signs (+) or (−) (bipolar injection, BMAOB). These charged sheets play a critical role in the formation and stabilization of flexo-dielectric walls as is schematically shown in figures 21 and 22. The model is based on (a) experimental observations regarding flexo-dielectric walls, (b) the Carr–Helfrich model for the Williams domains, (c) the Pikin model for the appearance of longitudinal hydrodynamic domains, (d) the Carr model [116, 117] for the appearance of walls at different circumstances, (e) understanding of double electric layers, the injection phenomenon, injection domains, etc. Evidently, flexo-dielectric domains are very complex and, which explains the peculiar character of these domains that have no counterpart among the other domain instabilities known for nematic liquid crystals.

Part of this experimental study was performed in the

Bayreuth University, Experimentalphysik V, Germany. We express our thanks to Professor I. Rehberg and to Dr F. Hörner for technical support. Support by the Bulgarian National Council 'Scientific Researches' at the Ministry of Education and Science, project P-823 is also acknowledged.

References

[1] Hinov, H., Vistin', L. K., and Magakova, Yu. G., 1978, *Kristallografiya*, **23,** 583 (*Sov. Phys. Crystallogr.*, **23,** 323).
[2] Hinov, H. P., and Vistin', L. K., 1979, *J. Phys., Paris.*, **40,** 269.
[3] Hinov, H. P., 1981, *Mol. Cryst. liq. Cryst.*, **74,** 39.
[4] Hinov, H. P., 1982, *Z. Naturforsch (a)*, **37,** 334.
[5] Hinov, H. P., 1982, *Mol. Cryst. liq. Cryst.*, **89,** 227.
[6] Weissflog, W., Pelzl, G., Kresse, H., and Demus, D., 1988, *Cryst. Res. Technol.*, **23,** 1259.
[7] Blinov, L. M., 1979, *J. Phys., Paris, Colloq.*, **C3 40,** C3–247.
[8] De Gennes, P.-G., 1974, *The Physics of Liquid Crystals* (Clarendon Press).
[9] Pikin, S. A., and Indenbom, V. I., 1975, *Kristallografiya*, **20,** 1127.
[10] Pikin, S., Ryschenkow, G., and Urbach, W., 1976, *J. Phys., Paris*, **37,** 241.
[11] Pikin, S. A., Chigrinov, V. G., and Indenbom, V. L., 1976, *Mol. Cryst. liq. Cryst.*, **37,** 313.
[12] Pikin, S. A., 1991, *Structural Transformations in Liquid Crystals* (New York: Gordon and Breach), Chap. 10.
[13] Guyon, E., Meyer, R., and Salan, J., 1979, *Mol. Cryst. liq. Cryst.*, **54,** 261.
[14] Lonberg, F., and Meyer, R., 1985, *Phys. Rev. Lett.*, **55,** 718.
[15] Meyer, R. B., 1969, *Phys. Rev. Lett.*, **22,** 918.
[16] Dmitriev, S. G., 1971, *Zh. eksp. teor. Fiz.*, **61**, 2049 (*Sov. Phys. JETP*, **34,** 1093).
[17] Fan, C., 1971, *Mol. Cryst. liq. Cryst.*, **13,** 9.
[18] Meyer, R. B., 1976, *Molecular Fluids: Structural Problems in Liquid Crystal Physics*, edited by R. Balian (New York: Gordon and Breach), pp 317–323.
[19] Derzhanski, A. I., Petrov, A. G., Khinov, KHR. P., and Markovski, B. L., 1974, *Bulg. J. Phys.*, **1,** 165.
[20] Derzhanski, A. I., Mitov, M. D., and Khinov, Khr. P., 1974, *C. r. Acad. Bulg. Sci.*, **27,** 453.
[21] Mitov, M. D., 1974, Diploma work, Sofia University, Bulgaria.
[22] Derzhanski, A. I., and Mitov, M. D., 1975, *C. r. Acad. Bulg. Sci.*, **28,** 1331.
[23] Petrov, A. G., 1974, PhD thesis, Institute of Solid State Physics, Bulgarian Academy of Sciences, Bulgaria.
[24] Derzhanski, A. I., and Petrov, A. G., 1979, *Acta Phys. Pol. A*, **55,** 747.
[25] Vistin', L. K., 1970, *Kristallografiya*, **15,** 594.
[26] Greubel, W., and Wolff, U., 1971, *Appl. Phys. Lett.*, **19,** 213.
[27] Bobylev, Y. P., and Pikin, S. A., 1977, *Zh. eksp. teor. Fiz.*, **72**, 369 (*Sov. Phys. JETP*, **45** 195).
[28] Bobylev, Y. P., Chigrinov, V. G., and Pikin, S. A., 1979, *J. Phys, Paris, Colloq.*, **40-C3,** C3–331.
[29] Barnik, M. I., Blinov, L. M., Trufanov, A. N., and Umanski, B. A., 1978, *J. Phys., Paris*, **39,** 417.
[30] Watson, P. K., Pollack, J. M., and Flannery, J. P., 1978, *Liquid Crystals and Ordered Fluids*, Vol. 3, edited by J. F. Johnson and R. S. Porter (Plenum) pp 421–442.
[31] Tanguay, A. R., Jr., Wu, C. S., Chavel, P., Strand, T. C., Sawchuk, A. A., and Soffer, B. H., 1983, *Opt. Eng.*, **22,** 687.
[32] Vistin', L. K., and Yakovenko, S. S., 1983, *Kristallografiya*, **28,** 992.
[33] Vistin', L. K., Chistyakov, I. G., Zharenov, R. P., and Yakovenko, S. S., 1976, *Kristallografiya*, **21**, 173 (*Sov. Phys. Crystallogr.*, **21,** 91).
[34] Vainstein, B. K., Chistyakov, I. G., Vistin', L. K., and Zharenov, R., 1976, *Bulg. Phys. J.*, **3,** 292.
[35] Barnik, M. I., Blinov, L. M., Trufanov, A. N., and Umanski, B. A., 1977, *Zh. eksp. teor. Fiz.*, **73**, 1936 (*Sov. Phys. JETP*, **46,** 1016).
[36] Barnik, M. I., Beljaev, S. V., Grebenkin, M. F., Rumjantsev, V. G., Seliverstov, V. A., Tsvetkov, V. A., and Shtykov, N. M., 1978, *Kristallografiya*, **23**, 805 (*Sov. Phys. Crystallogr.*, **23,** 451).
[37] Hinov, H. P., Bivas, I., Mitov, M. D., and Shoumarov, K. (in the press).
[38] Félici, N., 1969, *Rev. gen. Electr.*, **78,** 717.
[39] Koelmans, H., and van Boxtel, A. M., 1970, *Phys. Lett. A*, **32,** 32.
[40] Orsay Liquid Crystal Group, 1971, *Mol. Cryst. liq. Cryst.*, **12,** 251.
[41] Koelmans, H., and van Boxtel, A. M., 1971, *Mol. Cryst. liq. Cryst.*, **12,** 185.
[42] Lacroix, J.-C., and Tobazèon, R., 1972, *Appl. Phys. Lett.*, **20,** 251.
[43] Tobazèon, R., 1984, *J. Electrostat.*, **15,** 359.
[44] Turnbull, R. J., 1973, *J. Phys. D: appl. Phys.*, **6,** 1745.
[45] Honda, T., and Sasada, T., 1977, *Jpn. J. appl. Phys.*, **16,** 1775.
[46] Heilmeir, G., and Heyman, Ph., 1967, *Phys. Rev. Lett.*, **18,** 583.
[47] Cocco, R., Gáspard, F., and Hérino, R., 1979, *J. chim. Phys., Paris*, **76,** 383.
[48] Durand, G., Veyssie, M., Rondelez, F., and Lèger, L., 1970, *C. r. hebd. Séanc. Acad. Sci., Paris, B*, **270,** 97.
[49] Blinov, L. M., 1986, *Sci. Prog. Oxf.*, **70,** 263.
[50] Kai, S., Yoshitsune, N., and Hirakawa, K., 1975, *J. phys. Soc. Jpn.*, **38,** 1789.
[51] Vasilev, A. I., Balabanov, E. I., and Ushakov, V. M., 1980, *Advances in Liquid Crystal Research and Applications*, edited by L. Bata (Budapest: Pergamon Press), pp 583–587.
[52] Nehring, J., and Saupe, A., 1972, *J. chem. Soc. Faraday Trans. II*, **68,** 1.
[53] Demus, D., and Richter, L., 1978, *Textures in Liquid Crystals* (VEB Deutscher Verlag).
[54] Brière, G., Hérino, R., and Mondon, F., 1972, *Mol. Cryst. liq. Cryst.*, **19,** 157.
[55] Lomax, A., Hirasawa, R., and Bard, A. J., 1972, *J. electrochem. Soc.*, **119,** 1679.
[56] Denat, A., Gosse, B., and Gosse, J. P., 1973, *Chem. Phys. Lett.*, **18,** 235.
[57] Voinov, M., and Dunnett, J. S., 1973, *J. electrochem. Soc.*, **120,** 922.
[58] Sussman, A., 1974, *RCA Review*, **35,** 600.
[59] Fèlici, N., Gosse, B., and Gosse, J. P., 1976, *Rev. gen. Electr.*, **85,** 861.
[60] Hinov, H. P., and Shoumarov, K., 1993, in Abstracts

of International Congress Materials Science Technoloy, 20–23 October 1993, Sofia, Bulgaria, 5.3.
[61] KOVALEV, A. A., SYT'KO, L. V., MAZUR, I. P., NEKRASOV, G. L., and GROZHIK, V. A., 1977, *Kristallografiya*, **22,** 586 (*Sov. Phys. Crystallogr*, **22,** 334).
[62] ASLAKSEN, E. W., 1972, *J. appl. Phys.*, **43,** 776.
[63] LU, S., and JONES, D., 1970, *Appl. Phys. Lett.*, **16,** 484.
[64] ASSOULINE, G., HARENG, N., and LEIBA, E., 1971, *I.E.E.E. Trans. electron Devices*, **18,** 959.
[65] FÉLICI, N., and LACROIX, J.-C., 1971, *C. r. hebd. Séanc. Acad. Sci., Paris, B*, **273,** 65.
[66] SCHAPER, H., KÖSTLIN, H., and SCHEEDER, E., 1982, *Philips tech. Rev.*, **40,** 69.
[67] KOLODNER, P., WALDEN, R. W., PASSNER, A., and SURKO, C. M., 1986, *J. fl. Mech.*, **163,** 195.
[68] REHBERG, I., RASENAT, S., DE LA TORRE JUÁREZ, M., SCHÖPF, W., HÖRNER, F., AHLERS, G., and BRAND, H. R., 1991, *Phys. Rev. Lett.*, **67,** 596.
[69] RICHTER, H., RASENAT, S., and REHBERG, I., 1992, *Mol. Cryst. liq. Cryst.*, **222,** 219.
[70] RUDROFF, S., FRETTE, V., and REHBERG, I., 1999, *Phys. Rev. E*, **59,** 1814.
[71] DENNIN, M., 2000, *Phys. Rev. E*, **62,** 6780.
[72] JÉRÔME, B., 1991, *Rep. Prog. Phys.*, **54,** 391.
[73] SUGIMURA, A., LUCKHURST, G. R., and ZHONG-CAN, O.-Y., 1995, *Phys. Rev. E*, **52,** 681.
[74] BEICA, T., FRUNZA, S., MOLDOVAN, R., and STOENESCU, D. N., 1997, *Mol. Cryst. liq. Cryst.*, **301,** 39.
[75] ARONISHIDZE, S. N., BRODZELI, M. I., IVCHENKO, S. P., KUSHNIRENKO, M. N., MHATRISHVILI, M. D., TEDORASHVILI, K. G., and CHILAYA, G. S., 1975, *Fiz. Tv. Tela (USSR)*, **17,** 555.
[76] VAN ECK, D. C., and PERDECK, M., 1978, *Mol. Cryst. liq. Cryst. Lett.*, **49,** 39.
[77] PROUST, J. E., and TER-MINASSIAN-SARAGA, L., 1975, *J. Phys., Paris, Colloq.*, **36-C1,** C1–77.
[78] KIMURA, Y., NAKANO, K., KATO, T., and MORISHITA, S., 1994, *Wear*, **175,** 143.
[79] PIETSCH, U., BARBERKA, T. A., GENE, TH., and STÖMMER, R., 1997, *Nuovo Cim. D*, **19,** 393.
[80] ALLEN, C. M., and DRANGLIA, E., 1969, *Wear*, **14,** 363.
[81] PHILLIPS, P. L., RICHARDSON, R. M., ZARBAKNSH, A., and HASLAM, S. D., 1997, *Liq. Cryst.*, **23,** 699.
[82] RYSCHENKOW, G., and KLÉMAN, M., 1976, *J. chem. Phys.*, **64,** 404.
[83] GUYON, E., and URBACH, W., 1976, *Nonemissive Electrooptic Displays*, edited by A. Kmetz and F. K. von Willisen, pp 121–144.
[84] MARUSII, T. YA., REZNIKOV, YU. A., RESHETNYAK, V., SOSKIN, M. S., and KHIZHNYAK, A. I., 1986, *Zh. eksp. teor. Fiz*, **91,** 851.
[85] KLÉMAN, M., and WILLIAMS, C., 1973, *Phil. Mag. A*, **28,** 725.
[86] PORTE, G., 1976, *J. Phys., Paris*, **37,** 1245.
[87] PORTE, G., 1977, *J. Phys., Paris*, **38,** 509.
[88] KUTTY, T. R. N., and FISCHER, A. G., 1983, *Mol. Cryst. liq. Cryst.*, **99,** 301.
[89] KOEZUKA, H., KANEGAE, H., ONO, H., and SHIBAYAMA, K. J., 1982, *J. appl. Phys.*, **53,** 496.
[90] MEYER, R. B., 1973, *Solid State Commun.*, **12,** 585.
[91] WILLIAMS, C., VITEK, V., and KLÉMAN, M., 1973, *Solid State Commun.*, **12,** 581.
[92] PROST, J., and MARCEROU, J. P., 1977, *J. Phys., Paris*, **38,** 315.
[93] MARCEROU, J. P., and PROST, J., 1980, *Mol. Cryst. liq. Cryst.*, **58,** 259.
[94] GOOSSENS, W. J. A., 1989, *Liq. Cryst.*, **5,** 1083.
[95] HÉRINO, R. J., 1981, *J. appl. Phys.*, **52,** 3690.
[96] MCCLYMER, J. P., and LABES, M. M., 1987, *Mol. Cryst. liq. Cryst.*, **144,** 275.
[97] GOLOVANOV, A. V., KAZNACHEEV, A. V., and SONIN, A. S., 1998, *Izv. Akad. Nauk, Seria Fizika*, **62,** 1658.
[98] SCHWENK, N., and SPIESS, H. W., 1993, *J. Phys. II, Paris*, **3,** 865.
[99] MONZEN, K., HIRAOKA, K., UEMATSU, Y., and DATE, M., 1998, *Polym. J.*, **30,** 499.
[100] RICHARDSON, A. T., 1980, *Q. J. Mech. appl. Math.*, **33,** 277.
[101] DERZHANSKI, A., PETROV, A. G., and MITOV, M. D., 1978, *J. Phys., Paris*, **39,** 273.
[102] DERZHANSKI, A., and PETROV, A. G., 1980, *Advances in Liquid Crystal Research and Applications*, edited by L. Bata (Budapesta: Pergamon Press) pp. 515–521.
[103] MEYERHOFER, D., 1974, *RCA Rev.*, **35,** 434.
[104] IMAI, M., NAITO, H., OKUDA, M., and SUGIMURA, A., 1995, *Mol. Cryst. liq. Cryst.*, **259,** 37.
[105] SCHAPER, H., and SCHNEIDER, E., 1982, *J. electroanal. Chem.*, **137,** 39.
[106] SCHILLING, R. B., and SCHACHTER, H., 1967, *J. appl. Phys.*, **38,** 841.
[107] HAKEMI, H., and LABES, M. M., 1974, *J. chem. Phys.*, **61,** 4020.
[108] THURSTON, R. N., CHENG, J., MEYER, R. B., and BOYD, G. D., 1984, *J. appl. Phys.*, **56,** 263.
[109] DUBOIS-VIOLETTE, E., 1972, *J. Phys., Paris*, **33,** 95.
[110] ZAHN, M., 1976, *J. appl. Phys.*, **47,** 3122.
[111] NAKAGAWA, M., and AKAHANE, T., 1983, *J. phys. Soc. Jpn.*, **52,** 3773.
[112] NAKAGAWA, M., and AKAHANE, T., 1983, *J. phys. Soc. Jpn.*, **52,** 3782.
[113] LANGE, A., MÜLLER, R., and BEHN, U., 1996, *Z. Phys. B*, **100,** 477.
[114] NEVSKAYA, G. E., CHIGRINOV, V. G., DZENIS, S. F., and KORKISHKO, T. V., 1989, *Optika i Spectroscopia (USSR)*, **66,** 145.
[115] NEVSKAYA, G. E., CHIGRINOV, V. G., TICHOMIROV, I. V., DZENIS, S. F., and BERESNEV, G. A., 1989, *Izv. Akad. Nauk SSR (seria Fizicheskaya)*, **53,** 2016.
[116] CARR, E. F., 1978, *Liquid Crystals and Ordered Fluids*, Vol. 3, edited by J. F. Johnson and R. S. Porter, pp165–176.
[117] CARR, E. F., 1991, *Mol Cryst. liq. Cryst.*, **202,** 1.
[118] IGNER, D., and FREED, J. H. *Mol. Cryst. liq. Cryst.*, **101,** 301.
[119] BERRY, J. S., 1976, *Z. Ang. Math. Phys.*, **27,** 403.
[120] FLEURY, V., CHAZALVIEL, J.-N., and ROSSO, M., 1993, *Phys. Rev. E*, **48,** 1279.
[121] GRITZENKO, N. I., and MOSHEL, N. V., 1980, *Ukr. Fiz. Zh.*, **25,** 1830.
[122] BERESNEV, L. A., PFEIFFER, M., PIKIN, S., HAASE, W., and BLINOV, L., 1992, *Ferroelectrics*, **132,** 99.
[123] BERESNEV, L. A., SCHUMACHER, E., PIKIN, S. A., FAN, Z., OSTROVSKY, B. I., HILLER, S., ONOKHOV, A. P., and HAASE, W., 1995, *Jpn. J. appl. Phys.*, **34,** 2404.